Published for SISSA by Springer

Received: January 30, 2017
Revised: June 6, 2017
Accepted: August 2, 2017
Published: August 22, 2017

JHEP08(2017)091

Rare radiative charm decays within the standard model and beyond

Stefan de Boer and Gudrun Hiller

Fakultät für Physik, TU Dortmund,
Otto-Hahn-Str. 4, D-44221 Dortmund, Germany

E-mail: stefan.deboer@tu-dortmund.de, ghiller@physik.uni-dortmund.de

Abstract: We present standard model (SM) estimates for exclusive $c \to u\gamma$ processes in heavy quark and hybrid frameworks. Measured branching ratios $\mathcal{B}(D^0 \to (\phi, \bar{K}^{*0})\gamma)$ are at or somewhat exceeding the upper range of the SM and suggest slow convergence of the $1/m_D, \alpha_s$-expansion. Model-independent constraints on $|\Delta C| = |\Delta U| = 1$ dipole operators from $\mathcal{B}(D^0 \to \rho^0\gamma)$ data are obtained. Predictions and implications for leptoquark models are worked out. While branching ratios are SM-like CP asymmetries $\lesssim 10\%$ can be induced. In SUSY deviations from the SM can be even larger with CP asymmetries of $O(0.1)$. If Λ_c-baryons are produced polarized, such as at the Z-pole, an angular asymmetry in $\Lambda_c \to p\gamma$ decays can be studied that is sensitive to chirality-flipped contributions.

Keywords: Beyond Standard Model, Heavy Quark Physics

ArXiv ePrint: 1701.06392

https://doi.org/10.1007/JHEP08(2017)091

Contents

1 Introduction **1**

2 $D \to V\gamma$ in effective theory framework **3**
- 2.1 Generalities 3
- 2.2 Corrections 4
- 2.3 Contributions from $Q_8^{(\prime)}$ 7
- 2.4 Weak annihilation induced modes 8

3 SM phenomenology **8**

4 $D \to V\gamma$ beyond the Standard Model **12**
- 4.1 Model-independently 12
- 4.2 Leptoquark models 14
- 4.3 SUSY 17

5 On $\Lambda_c \to p\gamma$ **18**

6 Summary **19**

A Parameters **21**

B $D \to V$ form factors **22**

C $D \to V\gamma$ amplitudes in the hybrid approach **23**

D $C_7^{\rm eff}$ from $\langle Q_{3-6}\rangle$ at two-loop QCD **27**

1 Introduction

A multitude of radiative charm decays is accessible at current and future high luminosity flavor facilities [1, 2]. In anticipation of the new data we revisit opportunities to test the standard model (SM) with $c \to u\gamma$ transitions [3–10], complementing studies with dileptons, e.g., [11–13]. To estimate the beyond the standard model (BSM) reach we detail and evaluate exclusive $D_{(s)} \to V\gamma$ decay amplitudes, where V is a light vector meson. We employ two frameworks, one based on the heavy quark expansion and QCD, adopting expressions from b-physics [14], and a hybrid phenomenological one, updating [5, 6]. The latter combines chiral perturbation and heavy quark effective theory and vector meson dominance (VMD). Both frameworks have considerable systematic uncertainties, leaving individual charm branching ratios without clear-cut interpretation unless the deviation

JHEP08(2017)091

from the SM becomes somewhat obvious. On the other hand, considering several observables, correlations can shed light on hadronic parameters or on the electroweak model [7]. The interpretation of asymmetries is much easier, as (approximate) symmetries of the SM make them negligible compared to the experimental precision for a while. In particular, we discuss implications of the recent measurements by Belle [15]

$$\begin{aligned} \mathcal{B}(D^0 \to \rho^0\gamma) &= (1.77 \pm 0.30 \pm 0.07) \cdot 10^{-5}\,, \\ A_{CP}(D^0 \to \rho^0\gamma) &= 0.056 \pm 0.152 \pm 0.006\,, \end{aligned} \tag{1.1}$$

where the CP asymmetry A_{CP} is defined as[1]

$$A_{CP}(D \to V\gamma) = \frac{\Gamma(D \to V\gamma) - \Gamma(\bar{D} \to \bar{V}\gamma)}{\Gamma(D \to V\gamma) + \Gamma(\bar{D} \to \bar{V}\gamma)}\,. \tag{1.2}$$

We compare data (1.1) to the SM predictions and derive model-independent constraints on BSM couplings. We further discuss two specific BSM scenarios, leptoquark models and the minimal supersymmetric standard model with flavor mixing (SUSY). For the former we point out that large logarithms from the leading 1-loop diagrams with leptons and leptoquarks require resummation. The outcome is numerically of relevance for the interpretation of radiative charm decays.

We further obtain analytical expressions for the contributions from the QCD-penguin operators to the effective dipole coefficient at 2-loop QCD. This extends the description of radiative and semileptonic $|\Delta C| = |\Delta U| = 1$ processes at this order [3, 11, 17].

While one expects the heavy quark and α_s-expansion to perform worse than in b-physics an actual quantitative evaluation of the individual contributions in radiative charm decays has not been done to date. Our motivation is to fill this gap and detail the expansion's performance when compared to the hybrid model, and to data. In view of the importance of charm for probing flavor in and beyond the SM seeking after opportunities for any, possibly data-driven improvement of the theory-description is worthwhile.

The organization of this paper is as follows: in section 2 we calculate weak annihilation and hard scattering contributions to $D \to V\gamma$ decay amplitudes. In section 3 we present SM predictions for branching ratios and CP asymmetries in this approach and in the hybrid model. We present model-independent constraints on BSM physics and look into leptoquark models and SUSY within the mass insertion approximation in section 4. Section 5 is on $\Lambda_c \to p\gamma$ decays and the testability of a polarized Λ_c-induced angular asymmetry at future colliders [18, 19]. In section 6 we summarize. In appendix A and B we give the numerical input and $D \to V$ form factors used in our analysis. Amplitudes in the hybrid model are provided in appendix C. Details on the 2-loop contribution from QCD-penguin operators are given in appendix D.

[1] The CP asymmetry of $D^0 \to \rho^0\gamma$ is mostly direct, analogous to the time-integrated CP asymmetry in $D^0 \to K^+K^-$ [16]. We thank Alan Schwartz for providing us with this information. In this work, we refer to A_{CP} as the direct CP asymmetry, neglecting the small indirect contribution.

JHEP08(2017)091

2 $D \to V\gamma$ in effective theory framework

The effective weak Lagrangian and SM Wilson coefficients are discussed in section 2.1. We work out and provide a detailed breakdown of the individual contributions to $D \to V\gamma$ amplitudes in the heavy-quark approach. We work out weak annihilation and hard gluon exchange corrections in section 2.2, with contributions from the gluon dipole operator given in section 2.3. In section 2.4 we consider weak annihilation induced modes.

2.1 Generalities

The effective $c \to u\gamma$ weak Lagrangian can be written as [11]

$$\mathcal{L}_{\text{eff}}^{\text{weak}} = \frac{4G_F}{\sqrt{2}} \left(\sum_{q\in\{d,s\}} V_{cq}^* V_{uq} \sum_{i=1}^{2} C_i Q_i^{(q)} + \sum_{i=3}^{6} C_i Q_i + \sum_{i=7}^{8} \left(C_i Q_i + C_i' Q_i' \right) \right) , \tag{2.1}$$

where G_F is the Fermi constant, V_{ij} are CKM matrix elements and the operators read

$$\begin{aligned}
Q_1^{(q)} &= (\bar{u}_L \gamma_{\mu_1} T^a q_L)(\bar{q}_L \gamma^{\mu_1} T^a c_L), & Q_2^{(q)} &= (\bar{u}_L \gamma_{\mu_1} q_L)(\bar{q}_L \gamma^{\mu_1} c_L), \\
Q_3 &= (\bar{u}_L \gamma_{\mu_1} c_L) \sum_{\{q:m_q<\mu_c\}} (\bar{q}\gamma^{\mu_1} q), & Q_4 &= (\bar{u}_L \gamma_{\mu_1} T^a c_L) \sum_{\{q:m_q<\mu_c\}} (\bar{q}\gamma^{\mu_1} T^a q), \\
Q_5 &= (\bar{u}_L \gamma_{\mu_1}\gamma_{\mu_2}\gamma_{\mu_3} c_L) \sum_{\{q:m_q<\mu_c\}} (\bar{q}\gamma^{\mu_1}\gamma^{\mu_2}\gamma^{\mu_3} q), & Q_6 &= (\bar{u}_L \gamma_{\mu_1}\gamma_{\mu_2}\gamma_{\mu_3} T^a c_L) \sum_{\{q:m_q<\mu_c\}} (\bar{q}\gamma^{\mu_1}\gamma^{\mu_2}\gamma^{\mu_3} T^a q), \\
Q_7 &= \frac{e m_c}{16\pi^2} (\bar{u}_L \sigma^{\mu_1\mu_2} c_R) F_{\mu_1\mu_2}, & Q_7' &= \frac{e m_c}{16\pi^2} (\bar{u}_R \sigma^{\mu_1\mu_2} c_L) F_{\mu_1\mu_2}, \\
Q_8 &= \frac{g_s m_c}{16\pi^2} (\bar{u}_L \sigma^{\mu_1\mu_2} T^a c_R) G^a_{\mu_1\mu_2}, & Q_8' &= \frac{g_s m_c}{16\pi^2} (\bar{u}_R \sigma^{\mu_1\mu_2} T^a c_L) G^a_{\mu_1\mu_2},
\end{aligned} \tag{2.2}$$

where $F_{\mu\nu}, G^a_{\mu\nu}, a = 1, \ldots, 8$ denote the electromagnetic, gluonic field strength tensor, respectively, and T^a are the generators of QCD. In the following all Wilson coefficients are understood as evaluated at the charm scale μ_c of the order of the charm mass m_c, and $\mu_c = 1.27\,\text{GeV}$ unless otherwise explicitly stated.

For the SM Wilson coefficients of $Q_{1,2}$ and the effective coefficient of the chromomagnetic dipole operator at leading order in α_s one obtains [11, 17], respectively,

$$\begin{aligned}
C_1^{(0)} &\in [-1.28, -0.83]\,, \qquad C_2^{(0)} \in [1.14, 1.06]\,, \\
C_8^{(0)\text{eff}} &\in [0.47 \cdot 10^{-5} - 1.33 \cdot 10^{-5} i, 0.21 \cdot 10^{-5} - 0.61 \cdot 10^{-5} i]\,,
\end{aligned} \tag{2.3}$$

where μ_c is varied within $[m_c/\sqrt{2}, \sqrt{2} m_c]$. $C_8^{(0)\text{eff}}$ is strongly GIM suppressed in the SM and negligible therein. $C_1^{(0)}$ and the color suppressed coefficient of the weak annihilation contribution introduced in section 2.2 ,

$$\frac{4}{9} C_1^{(0)} + \frac{1}{3} C_2^{(0)} \in [-0.189, -0.018]\,, \tag{2.4}$$

are subject to a large scale-uncertainty. Note, at next-to leading order, $4/9\, C_1 + 1/3\, C_2 \in [-0.042, 0.092]$. In this work first (second) entries in intervals correspond to the lower (upper) value of μ_c within $[m_c/\sqrt{2}, \sqrt{2} m_c]$.

JHEP08(2017)091

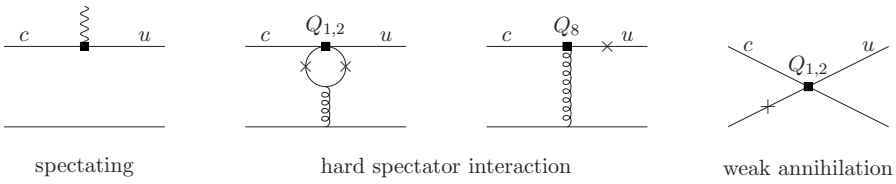

Figure 1. Diagrams driven by C_7^{eff}, weak annihilation and hard spectator interaction. The crosses indicate photon emission. Diagrams not shown are additionally power suppressed.

The effective coefficient of Q_7 including the matrix elements of Q_{1-6} at two-loop QCD, see [3, 11, 17] and appendix D for details, is in the range

$$C_7^{\text{eff}} \in [-0.00151 - (0.00556i)_{\text{s}} + (0.00005i)_{\text{CKM}}, -0.00088 - (0.00327i)_{\text{s}} + (0.00002i)_{\text{CKM}}] \tag{2.5}$$

and $C_7'^{\text{eff}} \sim m_u/m_c \simeq 0$. Here, we give contributions to the imaginary parts separately: the ones with subscript "s" correspond to strong phases, whereas the ones with label "CKM" stem from the weak phases in the CKM matrix. As a new ingredient we provide in this work the 2-loop QCD matrix element of Q_{3-6}, see appendix D for details. Numerically, $C_7^{\text{eff}}\big|_{\langle Q_{3-6}\rangle} \lesssim 10^{-6}$, that is, negligible due to small SM Wilson coefficients C_{3-6} and the GIM suppression.

The $D \to V\gamma$ decay rate can be written as [4]

$$\Gamma = \frac{m_D^3}{32\pi}\left(1 - \frac{m_V^2}{m_D^2}\right)^3 \left(|A_{\text{PC}}|^2 + |A_{\text{PV}}|^2\right) , \tag{2.6}$$

where the parity conserving (PC) and parity violating (PV) amplitudes read

$$A_{\text{PC/PV}} = \frac{\sqrt{\alpha_e 4\pi} G_F m_c}{2\sqrt{2}\pi^2}(A_7 \pm A_7')T \tag{2.7}$$

times $1/\sqrt{2}$ for $V^0 \in \{\rho^0, \omega\}$. Here, m_D and m_V denote the mass of the D and the vector meson, respectively, and $T = T_1(0) = T_2(0)$ is a $D \to V$ tensor form factor, see appendix B for details. We stress that the dominant SM contribution to $D_{(s)} \to V\gamma$ branching ratios is independent of T. Furthermore,

$$A_7^{(\prime)} = C_7^{(\prime)\text{eff}} + \dots , \tag{2.8}$$

where the ellipses indicate additional contributions from within and outside the SM. Corrections from within the SM are obtained in sections 2.2, 2.3 and 2.4. BSM coefficients and amplitudes are denoted by δC and $\delta A_7^{(\prime)}$, respectively. Note, A_7 and A_7' do not mix in eq. (2.6).

2.2 Corrections

In this section we calculate the hard spectator interaction (HSI) and weak annihilation (WA) contributions shown in figure 1 as corrections to the leftmost diagram in the figure.

JHEP08(2017)091

The leading ($\sim \alpha_s^1\,(\Lambda_{\rm QCD}/m_c)^0$) hard spectator interaction within QCD factorization adopted from b-physics [14] (also [20–22]) can be written as

$$C_7^{\rm HSI,V} = \frac{\alpha_s(\mu_h)}{4\pi}\left(\sum_{q\in\{d,s\}} V_{cq}^* V_{uq}\left(-\frac{1}{6}C_1^{(0)}(\mu_h) + C_2^{(0)}(\mu_h)\right) H_1^{(q)} + C_8^{(0)\rm eff}(\mu_h) H_8\right), \tag{2.9}$$

where we consistently use $C_{1,2,8}^{(0)}$ at leading order in α_s due to additional non-factorizable diagrams at higher order and $\mu_h \sim \sqrt{\Lambda_{\rm QCD} m_c}$. Furthermore,

$$\begin{aligned}
H_1^{(q)} &= \frac{4\pi^2 f_D f_V^\perp}{27 T m_D \lambda_D}\int_0^1 {\rm d}v\, h_V^{(q)}(\bar v)\,\Phi_{V\perp}(v),\\
h_V^{(q)} &= \frac{4m_q^2}{m_c^2\bar v^2}\left(\mathrm{Li}_2\left[\frac{2}{1-\sqrt{(\bar v - 4m_q^2/m_c^2 + i\epsilon])/\bar v}}\right] + \mathrm{Li}_2\left[\frac{2}{1+\sqrt{(\bar v - 4m_q^2/m_c^2 + i\epsilon])/\bar v}}\right]\right) - \frac{2}{\bar v},\\
H_8 &= -\frac{32\pi^2 f_D f_V^\perp}{27 T m_D \lambda_D}\int_0^1 {\rm d}v \frac{\Phi_{V\perp}(v)}{v},
\end{aligned} \tag{2.10}$$

$\bar v = 1 - v$ and $\mathrm{Li}_2[x] = -\int_0^x {\rm d}t \ln[1-t]/t$ and the decay constants $f_D, f_V^\perp$ are given in appendix A. We use $m_d = 0$. As $Q_8^{(\prime)}$-induced HSI contributions are negligible in the SM it follows that $C_7^{\rm HSI}$ is driven by $V_{cs}^* V_{us}$. The transverse distribution at leading twist is to first order in Gegenbauer polynomials

$$\Phi_{V\perp} = 6v\bar v\left(1 + a_1^{V\perp} 3(v-\bar v) + a_2^{V\perp}\frac{3}{2}\left(5(v-\bar v)^2 - 1\right)\right). \tag{2.11}$$

Numerical input on the Gegenbauer moments $a_{1,2}^{V\perp}$ is given in appendix A.

The parameter λ_D is defined as

$$\frac{m_D}{\lambda_D} = \int_0^1 {\rm d}\xi \frac{\Phi_D(\xi)}{\xi}, \tag{2.12}$$

that is the first negative moment of the leading twist distribution amplitude Φ_D of the light-cone momentum fraction ξ of the spectator quark within the D-meson. In b-physics, the first negative moment of the B-meson light-cone distribution amplitude, $\lambda_B^{\rm HQET} > 0.172\,{\rm GeV}$ at 90% C.L. [23], a positive light-cone wave function yields $\lambda_B^{\rm HQET} \leq 4/3\,\bar\Lambda$ [24] and by means of light-cone sum rules (LCSR) $\lambda_B^{\rm QCD} \lesssim \bar\Lambda$ [25, 26], where $\bar\Lambda = (m_B - m_b) + \mathcal{O}(\Lambda_{\rm QCD}^2/m_b)$ and $\lambda_B^{\rm HQET} > \lambda_B^{\rm QCD}$ at one-loop QCD [27]. We use $\lambda_D \sim \Lambda_{\rm QCD} \sim \mathcal{O}(0.1\,{\rm GeV})$.

Taking $\mu_h = 1\,{\rm GeV}$, varying the Gegenbauer moments and decay constants (but not the form factor T as it cancels in the amplitude) we find

$$\begin{aligned}
C_7^{{\rm HSI},\rho} &\in [0.00051 + 0.0014i, 0.00091 + 0.0020i]\cdot\frac{\rm GeV}{\lambda_D},\\
C_7^{{\rm HSI},\omega} &\in [0.00030 + 0.0010i, 0.00098 + 0.0020i]\cdot\frac{\rm GeV}{\lambda_D},\\
C_7^{{\rm HSI},K^{*+}} &\in [0.00032 + 0.0013i, 0.00096 + 0.0022i]\cdot\frac{\rm GeV}{\lambda_D}.
\end{aligned} \tag{2.13}$$

JHEP08(2017)091

We neglect isospin breaking in the Gegenbauer moments of the ρ. Contributions induced by $Q_8^{(\prime)}$ are discussed in section 2.3.

The leading ($\sim \alpha_s^0\,(\Lambda_{\rm QCD}/m_c)^1$) weak annihilation contribution to $D^0 \to (\rho^0,\omega)\gamma$, $D^+ \to \rho^+\gamma$ and $D_s \to K^{*+}\gamma$ can be inferred from b-physics [14, 28]. We obtain

$$\begin{aligned}
C_7^{\mathrm{WA},\rho^0} &= -\frac{2\pi^2 Q_u f_D f_{\rho^0}^{(d)} m_\rho}{T m_{D^0} m_c \lambda_D} V_{cd}^* V_{ud} \left(\frac{4}{9}C_1^{(0)} + \frac{1}{3}C_2^{(0)}\right), \\
C_7^{\mathrm{WA},\omega} &= \frac{2\pi^2 Q_u f_D f_{\omega}^{(d)} m_\omega}{T m_{D^0} m_c \lambda_D} V_{cd}^* V_{ud} \left(\frac{4}{9}C_1^{(0)} + \frac{1}{3}C_2^{(0)}\right), \\
C_7^{\mathrm{WA},\rho^+} &= \frac{2\pi^2 Q_d f_D f_\rho m_\rho}{T m_{D^+} m_c \lambda_D} V_{cd}^* V_{ud}\, C_2^{(0)}, \\
C_7^{\mathrm{WA},K^{*+}} &= \frac{2\pi^2 Q_d f_{D_s} f_{K^*} m_{K^*}}{T m_{D_s} m_c \lambda_D} V_{cs}^* V_{us}\, C_2^{(0)},
\end{aligned} \tag{2.14}$$

where $Q_u = 2/3$, $Q_d = -1/3$ and we consistently use $C_{1,2}^{(0)}$ at leading order in α_s. We neglect weak annihilation contributions from Q_{3-6} as the corresponding Wilson coefficients in the SM are strongly GIM suppressed. The minus sign for ρ^0 is due to isospin.

Varying the decay constants and μ_c within $[m_c/\sqrt{2}, \sqrt{2}m_c]$ we find

$$\begin{aligned}
C_7^{\mathrm{WA},\rho^0} &\in [-0.010, -0.0011] \cdot \frac{\mathrm{GeV}}{\lambda_D}, \\
C_7^{\mathrm{WA},\omega} &\in [0.0097, 0.0011] \cdot \frac{\mathrm{GeV}}{\lambda_D}, \\
C_7^{\mathrm{WA},\rho^+} &\in [0.029, 0.038] \cdot \frac{\mathrm{GeV}}{\lambda_D}, \\
C_7^{\mathrm{WA},K^{*+}} &\in [-0.034, -0.047] \cdot \frac{\mathrm{GeV}}{\lambda_D}.
\end{aligned} \tag{2.15}$$

Note that non-factorizable power corrections (inducing A_7') could in principle be calculated with LCSR, see, e.g., [29] and that non-local corrections to weak annihilation by means of QCD sum rules are additionally power suppressed [30].

To summarize, we observe the following hierarchies among the SM contributions to A_7

$$|C_7^{\mathrm{WA},V^+}| > |C_7^{\mathrm{WA},V^0}| \gtrsim |C_7^{\mathrm{HSI}}| > |C_7^{\mathrm{eff}}|. \tag{2.16}$$

The leading SM uncertainties are therefore those stemming from the WA-amplitudes, that is, the μ_c-scale and λ_D uncertainties, followed by the parameters entering HSI-amplitudes, i.e., Gegenbauer moments, decay constants and the μ_h-scale. The latter we fixed for simplicity.

Contributions to A_7' arise in the SM from a Q_2-induced quark loop with a soft gluon as a power correction [31]

$$C_7'^{(c\to u\gamma g)} \sim \frac{1}{3}C_2^{(0)} \left(V_{cd}^* V_{ud}\, f^{(c\to u\gamma g)}(m_d^2/m_c^2) + V_{cs}^* V_{us}\, f^{(c\to u\gamma g)}(m_s^2/m_c^2)\right) \frac{\Lambda_{\rm QCD}}{m_c}, \tag{2.17}$$

which is $\mathcal{O}(10^{-4})$ if the expansion coefficients of $f^{(c\to u\gamma g)}$ in m_q^2/m_c^2 are order one. Note that the $c \to u\gamma g$ process induces as well a contribution to A_7, and that the Q_1-induced

JHEP08(2017)091

quark loop is additionally color suppressed. Note also that $f^{(c\to u\gamma g)}$ could in principle be calculated with LCSR, see e.g., [29], yet α_s-corrections vanish at leading twist in the limit of massless quarks in the V-meson [32]. To be specific, and in absence of further calculations, we limit the size of the chirality-flipped SM amplitudes in our numerical analysis as

$$|A'_{7,\mathrm{SM}}/A_{7,\mathrm{SM}}| \lesssim 0.2\,, \tag{2.18}$$

and take the structure of the weak phases as in (2.17) into account.

2.3 Contributions from $Q_8^{(\prime)}$

We detail here the contributions from $Q_8^{(\prime)}$ to $c \to u\gamma$ modes. While in the SM they are negligibly small they can be relevant in BSM scenarios.

Numerically, we find for the $\langle Q_8^{(\prime)}\rangle$-induced hard spectator interaction of eq. (2.9)

$$\begin{aligned}
C_7^{(\prime)\mathrm{HSI},\rho}\big|_{\langle Q_8^{(\prime)}\rangle} &\in -\frac{\mathrm{GeV}}{\lambda_D}\cdot[0.031, 0.042]\cdot C_8^{(\prime)}\,,\\
C_7^{(\prime)\mathrm{HSI},\omega}\big|_{\langle Q_8^{(\prime)}\rangle} &\in -\frac{\mathrm{GeV}}{\lambda_D}\cdot[0.024, 0.040]\cdot C_8^{(\prime)}\,,\\
C_7^{(\prime)\mathrm{HSI},K^{*+}}\big|_{\langle Q_8^{(\prime)}\rangle} &\in -\frac{\mathrm{GeV}}{\lambda_D}\cdot[0.031, 0.039]\cdot C_8^{(\prime)}\,.
\end{aligned} \tag{2.19}$$

Note that QCD factorization breaks down at subleading power for $\langle Q_8\rangle$ hard spectator interaction due to a logarithmic singularity for a soft spectator quark [30].

Alternatively, LCSR yield the $\langle Q_8^{(\prime)}\rangle$ gluon spectator interaction (GSI) [33]

$$\begin{aligned}
C_7^{(\prime)\mathrm{GSI},\rho^0} &\in -[0.068 + 0.048i, 0.14 + 0.10i]\cdot C_8^{(\prime)}\,,\\
C_7^{(\prime)\mathrm{GSI},\omega} &\in -[0.018 - 0.024i, 0.036 - 0.048i]\cdot C_8^{(\prime)}\,,\\
C_7^{(\prime)\mathrm{GSI},\rho^+} &\in -[0.057 + 0.040i, 0.12 + 0.083i]\cdot C_8^{(\prime)}\,,\\
C_7^{(\prime)\mathrm{GSI},K^{*+}} &\in -[0.017 - 0.020i, 0.034 - 0.040i]\cdot C_8^{(\prime)}\,.
\end{aligned} \tag{2.20}$$

The contributions in eqs. (2.20) and (2.19) are similar in size for $\lambda_D \sim \mathcal{O}(0.1\,\mathrm{GeV})$. One may compare these to the $\langle Q_8^{(\prime)}\rangle$ induced contribution to eq. (2.5)

$$C_7^{(\prime)\mathrm{eff}}\big|_{\langle Q_8^{(\prime)}\rangle} \simeq (-0.12 - 0.17i)C_8^{(\prime)}\,. \tag{2.21}$$

BSM values $\delta C_8^{(\prime)} \lesssim 0.1$ can therefore lift the HSI/GSI contributions and the one to $C_7^{(\prime)\mathrm{eff}}$ such that

$$|C_7^{\mathrm{WA},V^+}| > |C_7^{\mathrm{WA},V^0}| \gtrsim |C_7^{\mathrm{HSI}}|, |C_7^{\mathrm{eff}}|\,. \tag{2.22}$$

JHEP08(2017)091

2.4 Weak annihilation induced modes

The contributions to A_7 of the weak annihilation induced decays $D^0 \to (\phi, \bar{K}^{*0}, K^{*0})\gamma$, $D^+ \to K^{*+}\gamma$ and $D_s \to \rho^+\gamma$ are obtained as follows

$$\begin{aligned}
C_7^{D^0\to\phi\gamma} &= \frac{2\pi^2 Q_u f_D f_\phi m_\phi}{T m_{D^0} m_c \lambda_D} V_{cs}^* V_{us} \left(\frac{4}{9} C_1^{(\bar{u}s)(\bar{s}c)} + \frac{1}{3} C_2^{(\bar{u}s)(\bar{s}c)}\right), \\
C_7^{D^0\to\bar{K}^{*0}\gamma} &= \frac{2\pi^2 Q_u f_D f_{K^*} m_{K^{*0}}}{T m_{D^0} m_c \lambda_D} V_{cs}^* V_{ud} \left(\frac{4}{9} C_1^{(\bar{u}d)(\bar{s}c)} + \frac{1}{3} C_2^{(\bar{u}d)(\bar{s}c)}\right), \\
C_7^{D^0\to K^{*0}\gamma} &= \frac{V_{cd}^* V_{us}}{V_{cs}^* V_{ud}} C_7^{D^0\to\bar{K}^{*0}\gamma}, \\
C_7^{D^+\to K^{*+}\gamma} &= \frac{2\pi^2 Q_d f_D f_{K^*} m_{K^{*+}}}{T m_{D^+} m_c \lambda_D} V_{cd}^* V_{us} C_2^{(\bar{u}s)(\bar{d}c)}, \\
C_7^{D_s\to\rho^+\gamma} &= \frac{2\pi^2 Q_d f_{D_s} f_\rho m_\rho}{T m_{D_s} m_c \lambda_D} V_{cs}^* V_{ud} C_2^{(\bar{u}d)(\bar{s}c)}.
\end{aligned} \tag{2.23}$$

Here we made the flavor structure of the Wilson coefficients explicit, however, since QCD is flavor symmetric, use $C_{1/2}^{(\bar{q}_1 q_2)(\bar{q}_3 c)} = C_{1/2}^{(0)}$. While the form factor T is process-dependent, it cancels together with m_c in the decay amplitude. Numerically, $\mathrm{GeV}/(m_c T) \sim 1$. Varying the decay constants and $\mu_c \in [m_c/\sqrt{2}, \sqrt{2} m_c]$ we find

$$\begin{aligned}
C_7^{D^0\to\phi\gamma} &\in [-0.016, -0.0013] \cdot \frac{\mathrm{GeV}}{\lambda_D} \frac{\mathrm{GeV}}{m_c T}, \\
C_7^{D^0\to\bar{K}^{*0}\gamma} &\in [-0.051, -0.0044] \cdot \frac{\mathrm{GeV}}{\lambda_D} \frac{\mathrm{GeV}}{m_c T}, \\
C_7^{D^0\to K^{*0}\gamma} &\in [0.0028, 0.00023] \cdot \frac{\mathrm{GeV}}{\lambda_D} \frac{\mathrm{GeV}}{m_c T}, \\
C_7^{D^+\to K^{*+}\gamma} &\in [0.0082, 0.0070] \cdot \frac{\mathrm{GeV}}{\lambda_D} \frac{\mathrm{GeV}}{m_c T}, \\
C_7^{D_s\to\rho^+\gamma} &\in [-0.16, -0.13] \cdot \frac{\mathrm{GeV}}{\lambda_D} \frac{\mathrm{GeV}}{m_c T}.
\end{aligned} \tag{2.24}$$

For $D^0 \to \phi\gamma$ additional contributions to the decay amplitude can arise, induced by $d\bar{d} + u\bar{u}$-admixture in the ϕ or rescattering [4]. Such effects can be parametrized by y as follows

$$\mathcal{A}(D^0 \to \phi\gamma) \simeq V_{cs}^* V_{us} a_\phi^{\mathrm{WA}} + y \left[V_{cd}^* V_{ud}\, a_{\rho^0}^{\mathrm{WA}} - V_{cs}^* V_{us}\, a_{\rho^0}^{\mathrm{HSI}} - a^{C_7^{\mathrm{eff}}}\right]. \tag{2.25}$$

To estimate A_{CP} we made CKM factors explicit except for the C_7^{eff}-induced term which can receive large BSM CP violating phases. The amplitudes correspond, in order of appearance, to $C_7^{D^0\to\phi\gamma}$, and the three contributions eqs. (2.14), (2.13) and (2.5) to $D^0 \to \rho^0\gamma$. Note the minus signs due do the $SU(3)$-composition. One obtains, model-independently,

$$A_{CP}(D^0 \to \phi\gamma) \simeq |y| A_{CP}(D^0 \to \rho^0\gamma) + \mathcal{O}(y^2). \tag{2.26}$$

3 SM phenomenology

We provide SM predictions for various $D_{(s)} \to V\gamma$ modes and compare to existing data. In addition to the QCD-based approach of the previous section we present branching ratios

JHEP08(2017)091

branching ratio	$D^0 \to \rho^0\gamma$	$D^0 \to \omega\gamma$	$D^+ \to \rho^+\gamma$	$D_s \to K^{*+}\gamma$
two-loop QCD	$(0.14 - 2.0) \cdot 10^{-8}$	$(0.14 - 2.0) \cdot 10^{-8}$	$(0.75 - 1.0) \cdot 10^{-8}$	$(0.32 - 5.5) \cdot 10^{-8}$
HSI+WA	$(0.11 - 3.8) \cdot 10^{-6}$	$(0.078 - 5.2) \cdot 10^{-6}$	$(1.6 - 1.9) \cdot 10^{-4}$	$(1.0 - 1.4) \cdot 10^{-4}$
hybrid	$(0.041 - 1.17) \cdot 10^{-5}$	$(0.042 - 1.12) \cdot 10^{-5}$	$(0.017 - 2.33) \cdot 10^{-4}$	$(0.053 - 1.54) \cdot 10^{-4}$
[5, 6]	$(0.1 - 1) \cdot 10^{-5}$	$(0.1 - 0.9) \cdot 10^{-5}$	$(0.4 - 6.3) \cdot 10^{-5}$	$(1.2 - 5.1) \cdot 10^{-5}$
[8]	$(0.1 - 0.5) \cdot 10^{-5}$	$0.2 \cdot 10^{-5}$	$(2 - 6) \cdot 10^{-5}$	$(0.8 - 3) \cdot 10^{-5}$
[9][a]	$3.8 \cdot 10^{-6}$	—	$4.6 \cdot 10^{-6}$	—
data[†]	$(1.77 \pm 0.31) \cdot 10^{-5}$	$< 2.4 \cdot 10^{-4}$	—	—

[a]Uncertainties not available. We take $a_1 = 1.3$ and $a_2 = -0.55$ [34].

Table 1. Branching ratios of $D \to V\gamma$ within the SM at two-loop QCD, from the hard spectator interaction plus weak annihilation and the hybrid approach. We vary the form factors, decay constants, lifetimes, Gegenbauer moments, relative strong phases and $\mu_c \in [m_c/\sqrt{2}, \sqrt{2}m_c]$. The branching ratios from the hard spectator interaction plus weak annihilation scale as $(0.1\,\text{GeV})/\lambda_D)^2$. Also given are data by the Belle [15] and the CLEO (at 90% CL) [35] collaborations as well as SM predictions from [5, 6], via pole diagrams and VMD [8] and QCD sum rules [9]. [†]Statistical and systematic uncertainties are added in quadrature.

in the phenomenological approach of [5, 6]. This model is a hybrid of factorization, heavy quark effective and chiral perturbation theory, where the $SU(3)$ flavor symmetry is broken by measured parameters. Compared to [5, 6] we rewrite the amplitudes in terms of newly measured parameters and vary (updated) parameters within uncertainties. Analytical expressions for the $D \to V\gamma$ amplitudes are provided in appendix C. The hierarchies of the various $D \to V\gamma$ amplitudes are predominantly set by CKM factors and large-N_C counting, taken care of in both the heavy quark and the hybrid frameworks.

The SM branching ratios and presently available data are given in table 1. We learn the following: the branching ratios induced by hard spectator interaction plus weak annihilation are typically smaller than (similar to) the ones obtained in the hybrid approach for neutral (charged) $c \to u\gamma$ modes. The branching ratio from two-loop QCD eq. (2.5) is subleading in each case. The branching ratios in the hybrid approach cover the ranges previously obtained in [5, 6, 8, 9]. The measured $D^0 \to \rho^0\gamma$ branching ratio is somewhat above the SM prediction in the hybrid model.

The branching ratios of $D \to \rho\gamma$ as a function of λ_D are shown in figure 2. The $D^+ \to \rho^+\gamma$ SM branching ratio is $\lesssim 2 \cdot 10^{-4}$, a measurement would constrain λ_D efficiently. Specifically, we find $\mathcal{B}(D^+ \to \rho^+\gamma) \simeq [44, 2900] \cdot \mathcal{B}(D^0 \to \rho^0\gamma)$ by means of hard spectator interaction plus weak annihilation and in the hybrid model $\mathcal{B}(D^+ \to \rho^+\gamma) \simeq [0.3, 280] \cdot \mathcal{B}(D^0 \to \rho^0\gamma)$. The $D^0 \to \rho^0\gamma$ branching ratio can be subject to stronger cancellations between the contributions in eq. (2.16) than in the hybrid model. Assuming that the phase of each amplitude $A^{\text{I/II/III}}_{\text{PV/PC}}$ is equal for $D^+ \to \rho^+\gamma$ and $D^0 \to \rho^0\gamma$ reduces the possible isospin breaking to $\mathcal{B}(D^+ \to \rho^+\gamma) \simeq [0.6, 140] \cdot \mathcal{B}(D^0 \to \rho^0\gamma)$. Note, isospin is already significantly broken by the lifetimes $\tau(D^0)/\tau(D^+) \simeq 0.4$ [36].

The uncertainties in the hybrid model are dominated by the relative strong phases, followed by the phenomenological fit coefficients $a_1 = 1.3 \pm 0.1$, $a_2 = -0.55 \pm 0.1$ [34] (also [37, 38]).

JHEP08(2017)091

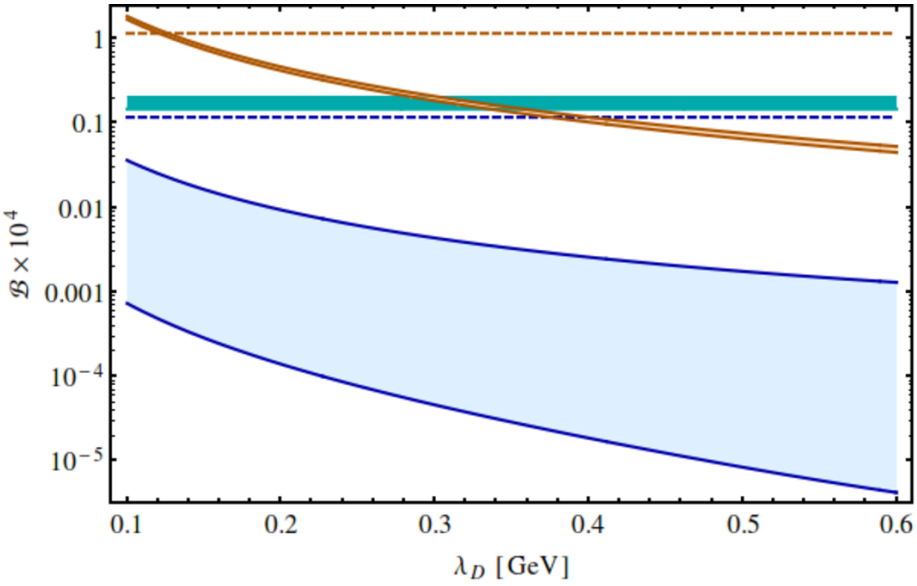

Figure 2. Branching ratios of $D \to \rho\gamma$ as a function of λ_D. The upper orange curves are for $D^+ \to \rho^+\gamma$ and the lower blue curves are for $D^0 \to \rho^0\gamma$. The solid curves represent the bands of two-loop QCD and hard spectator interaction plus weak annihilation, the dashed lines are the maximal predictions in the hybrid approach and the cyan band depicts the measured branching ratio [15]. We vary the form factors, decay constants, lifetimes, Gegenbauer moments, relative strong phases and $\mu_c \in [m_c/\sqrt{2}, \sqrt{2}m_c]$.

branching ratio	$D^0 \to \phi\gamma$	$D^0 \to \bar{K}^{*0}\gamma$	$D^0 \to K^{*0}\gamma$	$D^+ \to K^{*+}\gamma$	$D_s \to \rho^+\gamma$
WA	$(0.0074-1.2)\cdot 10^{-5}$	$(0.011-1.6)\cdot 10^{-4}$	$(0.032-4.4)\cdot 10^{-7}$	$(0.73-1.1)\cdot 10^{-5}$	$(1.8-2.9)\cdot 10^{-3}$
hybrid	$(0.24-2.8)\cdot 10^{-5}$	$(0.26-4.6)\cdot 10^{-4}$	$(0.076-1.3)\cdot 10^{-6}$	$(0.48-7.6)\cdot 10^{-6}$	$(0.11-1.3)\cdot 10^{-3}$
[5, 6]	$(0.4-1.9)\cdot 10^{-5}$	$(6-36)\cdot 10^{-5}$	$(0.03-0.2)\cdot 10^{-5}$	$(0.03-0.44)\cdot 10^{-5}$	$(20-80)\cdot 10^{-5}$
[8]	$(0.1-3.4)\cdot 10^{-5}$	$(7-12)\cdot 10^{-5}$	$0.1\cdot 10^{-6}$	$(0.1-0.3)\cdot 10^{-5}$	$(6-38)\cdot 10^{-5}$
[9][a]	—	$1.8\cdot 10^{-4}$	—	—	$4.7\cdot 10^{-5}$
Belle [15]†	$(2.76\pm 0.21)\cdot 10^{-5}$	$(4.66\pm 0.30)\cdot 10^{-4}$	—	—	—
BaBar [39]†[b]	$(2.81\pm 0.41)\cdot 10^{-5}$	$(3.31\pm 0.34)\cdot 10^{-4}$	—	—	—

[a] Uncertainties not available. We use $a_1 = 1.3$ and $a_2 = -0.55$ [34].
[b] We update the normalization [36].

Table 2. Branching ratios of $D^0 \to (\phi, \bar{K}^{*0}, K^{*0})\gamma$, $D^+ \to K^{*+}\gamma$ and $D_s \to \rho^+\gamma$ within the SM from weak annihilation and within the hybrid framework [5, 6] (appendix C). We vary the decay constants, lifetimes and $\mu_c \in [m_c/\sqrt{2}, \sqrt{2}m_c]$. The branching ratios induced by weak annihilation scale as $(0.1\,\text{GeV})/\lambda_D)^2$. Also given are available data by the Belle [15] and BaBar [39] collaborations, as well as SM predictions obtained in [5, 6], via pole diagrams and VMD [8] and QCD sum rules [9]. †Statistical and systematic uncertainties are added in quadrature.

The branching ratios of $D^0 \to (\phi, \bar{K}^{*0}, K^{*0})\gamma$, $D^+ \to K^{*+}\gamma$ and $D_s \to \rho^+\gamma$ are given in table 2. The measurements by Belle [15] and BaBar [39] of $\mathcal{B}(D^0 \to \bar{K}^{*0}\gamma)$ differ by 2.2σ, yet both are in the range of the hybrid model predictions. Interpreted in the QCD framework to the order we are working, $\mathcal{B}(D^0 \to (\bar{K}^{*0}, \phi)\gamma)$ data require a low value of λ_D

JHEP08(2017)091

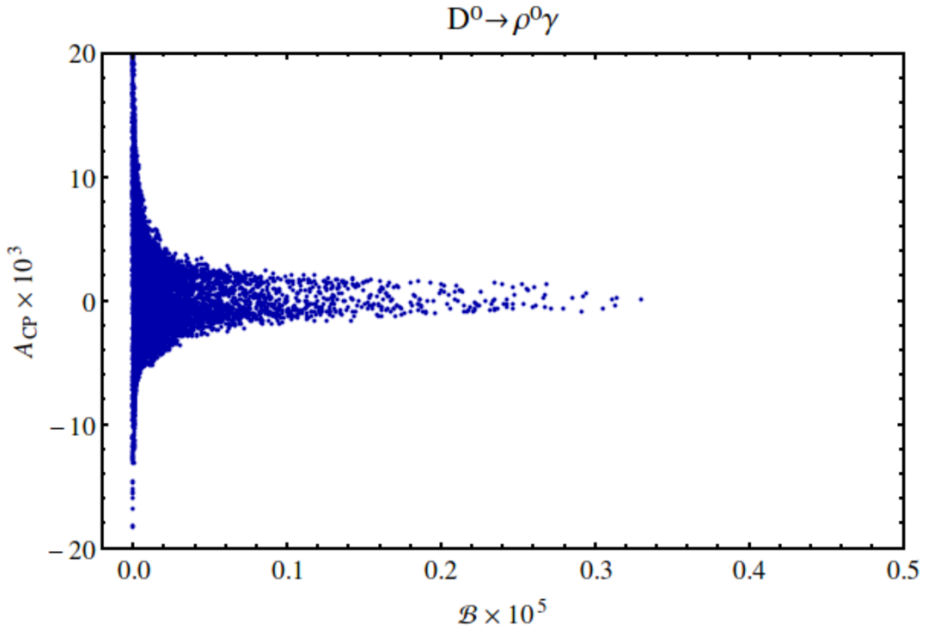

Figure 3. The CP asymmetry versus the branching ratio for $D^0 \to \rho^0\gamma$ decays in the SM. We vary the form factor, the two-loop QCD and hard spectator interaction plus weak annihilation within uncertainties, where $\lambda_D \in [0.1, 0.6]$ GeV, A_7'-contributions as in eq. (2.18) and relative strong phases. The measured A_{CP} eq. (1.1) covers the shown range, whereas the measured branching ratio at one σ is above it.

below 0.1 GeV or a low charm mass scale $\mu_c \sim m_c/2$, similar to $\mathcal{B}(D^0 \to \rho^0\gamma)$ data assuming the SM. Quite generally the deficiency in explaining the largely SM-dominated branching ratios in table 2 suggest slow convergence of the $1/m_D$, α_s-expansion. Measurements of branching ratios of color allowed D^+, D_s mesons could shed light on this, as here the scale uncertainty is smaller.

The CP asymmetry for $D^0 \to \rho^0\gamma$ within the SM in the heavy quark-based approach is shown in figure 3 as a function of the SM $D^0 \to \rho^0\gamma$ branching ratio. Within the SM $|A_{CP}| \lesssim 2 \cdot 10^{-2}$, if the branching ratio is $\gtrsim 10^{-9}$ and $|A_{CP}| \lesssim 2 \cdot 10^{-3}$, if $\mathcal{B}(D^0 \to \rho^0\gamma) \gtrsim 10^{-6}$, e.g., for $\lambda_D \lesssim 0.3$ GeV, and as measured (1.1) assuming the SM. $A_{CP}^{\rm SM}$ calculated in the hybrid model is $\lesssim 10^{-3}$, and vanishes in the SU(3)-limit. The SM CP asymmetry for $D^0 \to \omega\gamma$ is very similar to $A_{CP}(D^0 \to \rho^0\gamma)$; the CP asymmetries in the SM for the charged decays $D^+ \to \rho^+\gamma$ and $D_s \to K^{*+}\gamma$ are $\lesssim 2 \cdot 10^{-3}$ and $\lesssim 3 \cdot 10^{-4}$ in the heavy quark-based approach and the hybrid model, respectively. The enhancement of A_{CP} possible together with very low values of the branching ratio for D^0 decays originates from cancellations between different amplitudes.

The SM CP asymmetries for the pure WA modes $D^0 \to (\bar{K}^{*0}, K^{*0})\gamma$, $D^+ \to K^{*+}\gamma$ and $D_s \to \rho^+\gamma$ vanish due to a single weak phase cf. eq. (2.23) and appendix C. The decay $D^0 \to \phi\gamma$ is special as it can receive contributions at a fraction y similar to $D^0 \to \rho^0\gamma$ decays, and has therefore a finite CP asymmetry, estimated in equation (2.26). Taking into account a percent level $u\bar{u} + d\bar{d}$ content in the ϕ [36] values of A_{CP} up to $\mathcal{O}(10^{-4})$

JHEP08(2017)091

in the SM and up to $\mathcal{O}(10^{-3})$ in BSM models can arise in $D^0 \to \phi\gamma$ decays. Effects from rescattering at the ϕ-mass are roughly $y \lesssim 0.1$, hence corresponding CP asymmetries can reach $\mathcal{O}(10^{-3})$ in the SM and $\mathcal{O}(10^{-2})$ in BSM scenarios. The following asymmetries have been measured [15],

$$A_{CP}(D^0 \to \phi\gamma) = -0.094 \pm 0.066 \pm 0.001\,, \quad A_{CP}(D^0 \to \bar{K}^{*0}\gamma) = -0.003 \pm 0.020 \pm 0.000\,. \tag{3.1}$$

$A_{CP}(D^0 \to \phi\gamma)$ exhibits presently a mild tension with zero.

We stress that in our numerical evaluations we vary all relative strong (unknown) phases, including those between the WA+HSI contributions and the perturbative ones. In view of the appreciable uncertainties we refrain from putting an exact upper limit on the SM-induced CP asymmetries, but consider, to be specific, CP asymmetries at percent-level and higher as an indicator of BSM physics, consistent with [4]. This is supported by the large measured branching fractions, which indicate unsuppressed WA topologies. For the FCNC decays this suggests no large cancellations between the contributions in eq. (2.16), allowing for possible additional suppressions of CP asymmetries beyond CKM factors.

4 $D \to V\gamma$ beyond the Standard Model

In section 4.1 we work out model-independent constraints on $A_7^{(\prime)}$, $C_7^{(\prime)}$ and $C_8^{(\prime)}$. We calculate BSM Wilson coefficients within leptoquark models in section 4.2 and in SUSY in section 4.3, respectively, and discuss BSM implications.

4.1 Model-independently

Model-independently, from $\mathcal{B}(D^0 \to \rho^0\gamma)$ data, eq. (1.1), we obtain

$$|A_7^{(\prime)}, \delta A_7^{(\prime)}| \lesssim 0.5\,. \tag{4.1}$$

Constraints from $\mathcal{B}(D^+ \to \pi^+\mu^+\mu^-)$ data are similar [11]. These constraints prohibit that decays $D^+ \to \rho^+\gamma$ and $D_s \to K^{*+}\gamma$ are dominated by a BSM dipole contribution. Still, a sizable $\delta C_7^{(\prime)}$ can give the leading contribution to the neutral modes, causing their branching ratios to be very close to each other, $\mathcal{B}(D^0 \to \omega\gamma) \sim \mathcal{B}(D^0 \to \rho^0\gamma)$, similar to the SM, see table 1. Non-observation of this correlation indicates the presence of intermediate values of $\delta C_7^{(\prime)}$ [7].

BSM-induced CP asymmetries can reach $\mathcal{O}(0.1)$. Hence, current data on $A_{CP}(D^0 \to \rho^0\gamma)$ are too uncertain to provide further constraints. There is essentially no BSM pattern for CP asymmetries apart from their sign. Turning this around, it is possible to have a sizable value of A_{CP} in one mode but a small one in another.

To illustrate the impact of improved measurements of the $D^0 \to \rho^0\gamma$ branching ratio and CP asymmetry, we assume hypothetical data with a factor four reduced statistical uncertainty of the current measurements with central values kept [15], that is,

$$A_{CP}^{(\text{hypothetical})}(D^0 \to \rho^0\gamma) = 0.056 \pm 0.038, \;\; \mathcal{B}^{(\text{hypothetical})}(D^0 \to \rho^0\gamma) = (1.77 \pm 0.10) \cdot 10^{-5}\,. \tag{4.2}$$

JHEP08(2017)091

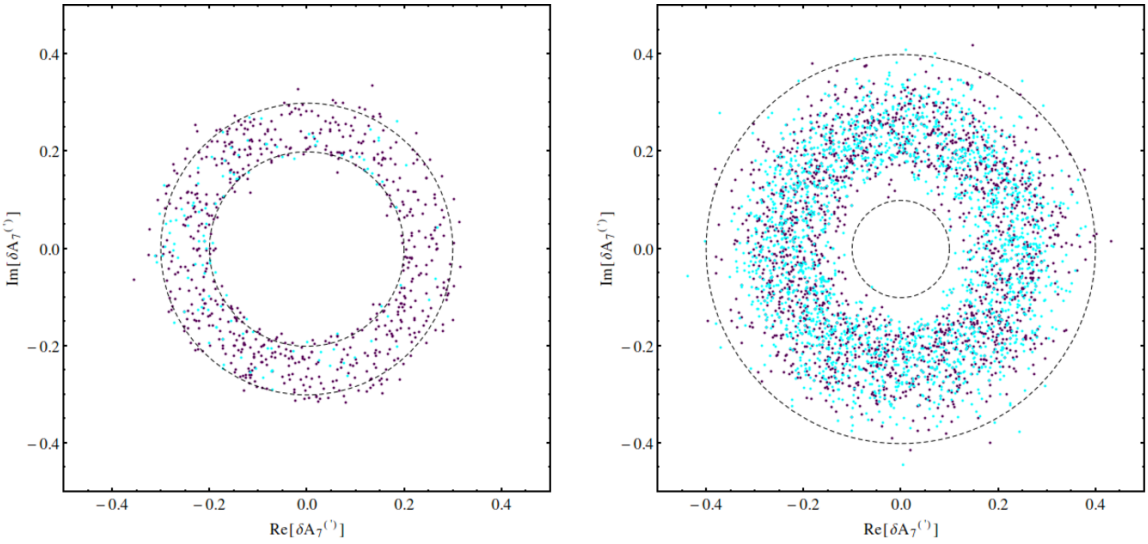

Figure 4. Projected model-independent constraints on $(\mathrm{Re}[\delta A_7], \mathrm{Im}[\delta A_7])$ (purple) and $(\mathrm{Re}[\delta A_7'], \mathrm{Im}[\delta A_7'])$ (cyan), from eq. (4.2) for the heavy quark-based approach (left plot) and the hybrid model (right plot). The dashed circles show $|\delta A_7^{(\prime)}| = 0.2, 0.3$ (left plot) and $|\delta A_7^{(\prime)}| = 0.1, 0.4$ (right plot) to guide the eye. We vary the form factor, the two-loop QCD, the hard spectator interaction plus weak annihilation coefficients, where $\lambda_D \in [0.1, 0.6]\,\mathrm{GeV}$ and eq. (2.18) (left plot) and amplitudes in the hybrid model (right plot) within uncertainties and relative phases.

In figure 4 corresponding 1 sigma-constraints are shown. The ones for A_7 (purple) and A_7' (cyan) are similar. The bounds are stronger for the QCD-based framework, roughly $0.2 \lesssim |\delta A_7^{(\prime)}| \lesssim 0.3$, $|\mathrm{Im}[\delta A_7^{(\prime)}]| \gtrsim \mathcal{O}(0.001)$ (plot to the left) than for the hybrid one, $0.1 \lesssim |\delta A_7^{(\prime)}| \lesssim 0.4$, $|\mathrm{Im}[\delta A_7]| \gtrsim \mathcal{O}(0.001)$, $|\mathrm{Im}[\delta A_7']| \gtrsim \mathcal{O}(0.0001)$ (plot to the right), improving on the present situation, eq. (4.1). In the hybrid model the unknown strong phases prohibit a meaningful calculation of A_7/A_7' in the SM [6]. We therefore do not employ constraints from eq. (2.18) in this model.

We consider now the impact of the chromomagnetic dipole operator. The CP asymmetry induced by the matrix element of $Q_8^{(\prime)}$ estimated within LCSR reads [40]

$$A_{CP}\big|_{\langle Q_8, Q_8'\rangle} \sim -\mathrm{Im}\left[2C_8 + \frac{1}{2}C_8'\right], \tag{4.3}$$

which, together with data eq. (1.1), yields the constraint $|\mathrm{Im}[\delta C_8^{(\prime)}]| \lesssim \mathcal{O}(0.1)$. CP violation in charm is also constrained by data on $\Delta A_{CP} = A_{CP}(K^+K^-) - A_{CP}(\pi^+\pi^-) \sim -2\mathrm{Im}[C_8 - C_8'] \sin\delta_{KK-\pi\pi}$ [40, 41], where $\Delta A_{CP} = -0.00134 \pm 0.00070$ [42]. To escape a potentially strong bound on $\mathrm{Im}[\delta C_8 - \delta C_8']$ at permille level requires suppression by the unknown strong phase difference between K^+K^- and $\pi^+\pi^-$, $\delta_{KK-\pi\pi}$, or some cancellations between different sources of BSM CP violation.

The Wilson coefficients $\delta C_7^{(\prime)}(M)$ and $\delta C_8^{(\prime)}(M)$ are generically related within BSM models, where M denotes the matching scale, of the order of the electroweak scale or higher.

JHEP08(2017)091

In addition, $\delta C_{7,8}^{(\prime)}$ are related by the renormalization group evolution. At one-loop QCD

$$\delta C_7^{(\prime)}(\mu_c) = a_7\, \delta C_7^{(\prime)}(M) + \frac{16}{3}(a_7 - a_8)\delta C_8^{(\prime)}(M)\,, \qquad \delta C_8^{(\prime)}(\mu_c) = a_8\, \delta C_8^{(\prime)}(M)\,, \tag{4.4}$$

where

$$\begin{aligned} a_7 &= \left(\frac{\alpha_s(M)}{\alpha_s(\mu_t)}\right)^{16/21} \left(\frac{\alpha_s(\mu_t)}{\alpha_s(\mu_b)}\right)^{16/23} \left(\frac{\alpha_s(\mu_b)}{\alpha_s(\mu_c)}\right)^{16/25}, \\ a_8 &= \left(\frac{\alpha_s(M)}{\alpha_s(\mu_t)}\right)^{14/21} \left(\frac{\alpha_s(\mu_t)}{\alpha_s(\mu_b)}\right)^{14/23} \left(\frac{\alpha_s(\mu_b)}{\alpha_s(\mu_c)}\right)^{14/25}. \end{aligned} \tag{4.5}$$

Including effects of $\langle Q_8^{(\prime)}\rangle$, eq. (2.21), and neglecting SM contributions, we find

$$\delta A_7^{(\prime)}\big|_{Q_8^{(\prime)}} \simeq 0.4\, \delta C_7^{(\prime)}(1\,\text{TeV}) - (0.3 + 0.1i)\, \delta C_8^{(\prime)}(1\,\text{TeV})\,. \tag{4.6}$$

Additionally, we find the mixing via $Q_{3-6}^{(\prime)}$, [17] and appendix D, neglecting the SM,

$$\begin{aligned} \delta A_7^{(\prime)}\big|_{Q_{3-6}^{(\prime)}} \simeq{}& (0.3 - 0.1i)\, \delta C_3^{(\prime)}(1\,\text{TeV}) + (0.7 + 0.1i)\, \delta C_4^{(\prime)}(1\,\text{TeV}) \\ &+ (-3.5 - 1.9i)\, \delta C_5^{(\prime)}(1\,\text{TeV}) + (-0.6 + 1.1i)\, \delta C_6^{(\prime)}(1\,\text{TeV})\,. \end{aligned} \tag{4.7}$$

BSM effects from 4-quark operators are, however, strongly constrained by ϵ'/ϵ and $D - \bar{D}$ mixing, and we do not consider this possibility any further.

To compete with the SM $\delta C^{(\prime)}(M) \sim \mathcal{O}(0.1 - 1)$ is required, which is difficult to achieve given the loop factor and possible further flavor suppressions. However, BSM CP asymmetries around a percent require $\delta C(M)$ of a few permille only but need sizable phases. The impact of $\delta C'(M)$ on CP asymmetries is suppressed due to the hierarchy between the left and right-chiral SM contribution and since there is no interference between them in the branching ratio.

4.2 Leptoquark models

We consider contributions from scalar $S_{1,2,3}$ and vector $V_{2,3}, \tilde{V}_{1,2}$ leptoquark representations to $c \to u\gamma$ processes, see [11, 43–46] for Lagrangians and details.[2] In this section we denote by M the mass of the leptoquark and by $\lambda_{L/R}$ leptoquark couplings to left-/right-handed leptons. For vector-like couplings we omit the chirality index.

Due to the light leptons in the loop $\delta_{LQ} C_{1-8}^{(\prime)}(\mu = M) = 0$, however, the following vector (V) and scalar (S) operators are induced at tree-level

$$O_V^{(l)} = (\bar{u}_L \gamma_\mu l_L)(\bar{l}_L \gamma^\mu c_L)\,, \quad O_S^{(l)} = (\bar{u}_L l_R)(\bar{l}_L c_R) \tag{4.8}$$

plus chirality-flipped contributions. Here, schematically, $C_V^{(l)}(\mu = M) = \lambda\lambda^*/M^2$ and $C_S^{(l)}(\mu = M) = \lambda_R \lambda_L^*/M^2$. At one-loop QCD $C_V^{(l)}(\mu_c) = C_V^{(l)}(M)$ and $C_S^{(l)}(\mu) =$

[2] In [11] the notation differs from the one used here by means of charge conjugated fields. Here we write $q \to \bar{q}^C$ for the leptoquarks S_1, S_3, V_2 and $\tilde{V}_2$ in [11] and adjust their couplings correspondingly. Moreover, here an additional sign for all vector leptoquarks is accounted for. Conclusions in [11] are unaffected.

JHEP08(2017)091

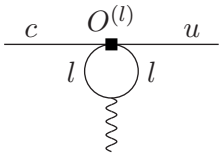

Figure 5. Diagram inducing $c \to u\gamma$ within leptoquark models.

LQ	κ	κ'	ν	ν'
S_1	$\lambda_R^{(cl)}(\lambda_R^{(ul)})^*$	$\lambda_L^{(cl)}(\lambda_L^{(ul)})^*$	$\lambda_L^{(cl)}(\lambda_R^{(ul)})^*$	$\lambda_R^{(cl)}(\lambda_L^{(ul)})^*$
S_2	$(\lambda_R^{(cl)})^*\lambda_R^{(ul)}$	$(\lambda_L^{(cl)})^*\lambda_L^{(ul)}$	$(\lambda_L^{(cl)})^*\lambda_R^{(ul)}$	$(\lambda_R^{(cl)})^*\lambda_L^{(ul)}$
S_3	—	$\lambda^{(cl)}(\lambda^{(ul)})^*$	—	—
$\tilde{V}_1$	$(\lambda^{(cl)})^*\lambda^{(ul)}$	—	—	—
V_2	$\lambda^{(cl)}(\lambda^{(ul)})^*$	—	—	—
$\tilde{V}_2$	—	$\lambda^{(cl)}(\lambda^{(ul)})^*$	—	—
V_3	—	$(\lambda^{(cl)})^*\lambda^{(ul)}$	—	—

Table 3. Couplings to equations (4.9) and (4.11) with flavor indices made explicit.

$(\alpha_s(M)/\alpha_s(\mu))^{8/(2\beta_0)}\, C_S^{(l)}(M)$, where $\beta_0 = 11 - 2/3\, n_f$ and n_f is the number of active flavors, hence thresholds need to be taken into account.

At the scale $\mu = m_\tau$ the τ lepton is to be integrated out. Since numerically $m_\tau \sim \sqrt{2} m_c$ we include the tau-loop contributions in the matrix element of $O_{V,S}^{(l)}$, see figure 5. The contribution of $O_V^{(l)(\prime)}$ vanishes to all orders in α_s. From the matrix element of $O_S^{(l)(\prime)}$ we obtain

$$\delta_{LQ} A_7^{(\prime)}(\mu_c) = \frac{-Q_l}{4\sqrt{2} G_F} \frac{m_l}{m_c} \left(1 + \ln \frac{\mu_c^2}{m_l^2}\right) \left(\frac{\alpha_s(M)}{\alpha_s(\mu_t)}\right)^{12/21} \left(\frac{\alpha_s(\mu_t)}{\alpha_s(\mu_b)}\right)^{12/23} \left(\frac{\alpha_s(\mu_b)}{\alpha_s(\mu_c)}\right)^{12/25} \frac{\nu^{(\prime)}}{M^2}. \tag{4.9}$$

Here, Q_l denotes the electric charge of the leptons. The couplings $\nu^{(\prime)}$ within leptoquark models are given in table 3. Note that $\delta_{LQ} A_8^{(\prime)}(\mu_c)$ is additionally $\alpha_e/(4\pi)$ suppressed and will be neglected throughout.

Constraints on τ couplings are worked out and given in table 4, where we followed [11] and used [36]. The representations $V_{2,3}$ turn about to be not relevant for $c \to u\gamma$ decays and no constraints are given. Note that $\mathcal{B}(D^0 \to \rho^0\gamma)$ yields no constraint for $\lambda \lesssim 1$. Lepton flavor violating τ decays constrain couplings with a τ and a light lepton; we do not take these constraints into account as they can be evaded with a flavor suppression of the light leptons.

Numerically, we find for $l = \tau$ and the constraints given in table 4

$$|\delta_{LQ} A_7^{(\prime)}(\mu_c)| \simeq 0.01 |\lambda_R \lambda_L^*| (\mathrm{TeV}/M)^2 \lesssim \mathcal{O}(10^{-3}), \tag{4.10}$$

for the chirality-flipping contributions $\propto m_\tau/m_c$ of the leptoquark representations S_1, S_2. As we are interested in CP asymmetries we allow here for a mild suppression of the real parts of $\lambda_R \lambda_L^*$ relative to the imaginary ones, the latter of which are weaker constrained

JHEP08(2017)091

couplings/mass	constraint	observable
$\lvert\lambda^{(u\tau)}_{S_3}\rvert$	$\sim [0.0, 0.2]$	$\tau^- \to \pi^- \nu_\tau$
$\mathrm{Re}[\lambda^{(u\tau)}_{SR}(\lambda^{(u\tau)}_{SL})^*]$	$\sim [0.00, 0.09]$	
$\mathrm{Re}[\lambda^{(u\tau)}_{S_1L,S_3}(\lambda^{(c\tau)}_{S_1L,S_3})^*]$	$\sim [-0.2, 0.2]$	$\tau^- \to K^- \nu_\tau$
$\mathrm{Re}[\lambda^{(u\tau)}_{SR}(\lambda^{(c\tau)}_{SL})^*]$	$\sim [-0.07, 0.04]$	
$\lvert\mathrm{Im}[\lambda^{(u\tau)}_{SR}(\lambda^{(c\tau)}_{SL})^*]\rvert$	$\sim [0.0, 0.7]$	
$\lvert\mathrm{Re}[\lambda^{(u\tau)}_{SL,SR}(\lambda^{(c\tau)}_{SL,SR})^*]\rvert$	$\sim [0, 0.02]$	Δm_{D^0}
$\lvert\mathrm{Re}[\lambda^{(u\tau)}_{S_3}(\lambda^{(c\tau)}_{S_3})^*]\rvert$	$\sim [0, 0.007]$	
$\mathrm{Re}[\lambda^{(u\tau)}_{SR}(\lambda^{(c\tau)}_{SL})^*]$	$\lesssim 0.3$	$D^+ \to \tau^+ \nu_\tau$
$\mathrm{Re}[\lambda^{(c\tau)}_{SR}(\lambda^{(c\tau)}_{SL})^*]$	$\sim [-1, 0.09]$	$D_s \to \tau^+ \nu_\tau$
$\lvert\lambda^{(c\tau)}_{S_3}\rvert$	$\sim [0.0, 0.4]$	
$\lvert\lambda^{(u\tau)}_{S_1L,S_3}\lambda^{(c\tau)}_{S_1L,S_3}\rvert$	$\lesssim 4 \cdot 10^{-4}$	$(K^+ \to \pi^+ \bar{\nu}\nu)/(K^+ \to \pi^0 \bar{e}\nu)$

Table 4. Scalar leptoquark constraints on couplings to τ's scaling as TeV$/M$ and $\sqrt{\text{TeV}/M}$ for Δm_{D^0}. The kaon constraints are found via [47]. The vector ($\tilde{V}_{1,2}$) leptoquark couplings are unconstrained by the above observables.

experimentally. At this order, all other leptoquark contributions vanish. Finite contributions are, however, expected for other couplings and representations at two-loop QED. The corresponding leading order calculation in α_e is similar to the $\langle Q_2 \rangle$ two-loop QCD calculation in [3, 48], and beyond the scope of our work.

Instead we employ expressions from [49] for fixed order results in the full SM plus scalar (S) and gauge vector (V) leptoquark theory and obtain, respectively,

$$\begin{aligned}
\delta_{\langle S\rangle} A_7^{(\prime)}(\mu_c) &= -\frac{1}{4\sqrt{2}G_F m_c}\left(\kappa^{(\prime)}\left(Q_l k_1 + Q_S \bar{k}_1\right) + \nu^{(\prime)}\left(Q_l k_3 + Q_S \bar{k}_3\right)\right), \\
\delta_{\langle V\rangle} A_7^{(\prime)}(\mu_c) &= -\frac{1}{4\sqrt{2}G_F m_c}\kappa^{(\prime)}(Q_l y_1 + Q_V \bar{y}_1),
\end{aligned} \tag{4.11}$$

where the electric charge of the leptoquark $Q_{S,V}$ is fixed by charge conservation,

$$\begin{aligned}
k_1 &= \frac{m_c}{M^2}\frac{1}{6}, \qquad \bar{k}_1 = \frac{m_c}{M^2}\frac{1}{12}, \qquad k_3 = \frac{m_l}{M^2}\left(\frac{-3}{2} - \ln\frac{m_l^2}{M^2}\right), \qquad \bar{k}_3 = \frac{m_l}{M^2}\frac{1}{2}, \\
y_1 &= \frac{m_c}{M^2}\frac{-2}{3}, \qquad \bar{y}_1 = \frac{m_c}{M^2}2
\end{aligned} \tag{4.12}$$

and the couplings $\nu^{(\prime)}$, $\kappa^{(\prime)}$ are given in table 3. Note the large logarithm $\ln[m_l^2/M^2]$ proportional to m_l in the scalar contribution. It resembles the (resummed) logarithm in equation (4.9) and originates from the inclusion of a light mass, which we drop in the following. The resulting coefficients are worked out numerically in table 5. There are no contributions to $A_7^{(\prime)}$ in leptoquark models $V_{2,3}$. For $l = e, \mu$ we find with the constraints given in [11] that $|\delta_{\langle \tilde{V}_1\rangle} A_7|_{e,\mu} \lesssim 0.002$ and $|\delta_{\langle \tilde{V}_2\rangle} A_7'|_{e,\mu} \lesssim 0.002$. The contributions from scalar leptoquarks are negligible, $|\delta_{\langle S_{1,2,3}\rangle} A_7^{(\prime)}|_{e,\mu} \lesssim \mathcal{O}(10^{-5})$.

JHEP08(2017)091

LQ	$\delta_{\langle LQ\rangle}A_7$	$\delta_{\langle LQ\rangle}A_7'$
S_1	$-0.003\,\lambda_R^{(cl)}(\lambda_R^{(ul)})^*$	$-0.003\,\lambda_L^{(cl)}(\lambda_L^{(ul)})^*$
S_2	$0.005\,(\lambda_R^{(cl)})^*\lambda_R^{(ul)}$	$0.006\,(\lambda_L^{(cl)})^*\lambda_L^{(ul)}$
S_3	0	$-0.002\,\lambda^{(cl)}(\lambda^{(ul)})^*$
$\tilde{V}_1$	$0.04\,(\lambda^{(cl)})^*\lambda^{(ul)}$	0
$\tilde{V}_2$	0	$-0.02\,\lambda^{(cl)}(\lambda^{(ul)})^*$
$V_{2,3}$	0	0

Table 5. Leptoquark induced coefficients for $M = 1\,\text{TeV}$ from eq. (4.11) and $m_l = 0$. For $M \to 10\,\text{TeV}$ the effective coupling scales as $\lambda^{(cl)}\lambda^{(ul)}/(M = 1\,\text{TeV})^2 \to 0.9\,\lambda^{(cl)}\lambda^{(ul)}/(M = 10\,\text{TeV})^2$.

The τ couplings for S_3 and S_{1L} receive their strongest constraint from K decays, $|\delta_{\langle S_{1L,3}\rangle}A_7'|_\tau \lesssim \mathcal{O}(10^{-6})$. All other bounds in table 4 can be escaped with phase-tuning $\text{Im}[\lambda^{(u\tau)}(\lambda^{(c\tau)})^*] \gg \text{Re}[\lambda^{(u\tau)}(\lambda^{(c\tau)})^*]$. Corresponding BSM coefficients δA_7 and $\delta A_7'$ can be read off from table 5 for $\lambda_{L,R}^{(q\tau)} \lesssim 1$. Assuming instead $\text{Im}[\lambda^{(u\tau)}(\lambda^{(c\tau)})^*] \lesssim \text{Re}[\lambda^{(u\tau)}(\lambda^{(c\tau)})^*]$, one obtains from D-mixing $|\delta_{\langle S_{1L,2L,2R}\rangle}A_7^{(\prime)}|_\tau \lesssim \mathcal{O}(10^{-4})$. For vector leptoquarks we find $|\delta_{\langle \tilde{V}_2\rangle}A_7'|_\tau \lesssim 0.02$ and $|\delta_{\langle \tilde{V}_1\rangle}A_7|_\tau \lesssim 0.04$. Note, $\delta_{\langle S_1,S_2\rangle}A_7^{(\prime)}|_\tau$ from chirality-flipping contributions without resummation would be about one order of magnitude larger than eq. (4.10).

To summarize, within leptoquark models the $c \to u\gamma$ branching ratios are SM-like with CP asymmetries at $\mathcal{O}(0.01)$ for $S_{1,2}$ and $\tilde{V}_2$ and SM-like for S_3. On the other hand, in model $\tilde{V}_1$ $A_{CP} \lesssim \mathcal{O}(10\%)$. The largest effects arise from τ-loops.

4.3 SUSY

Here we consider effects within SUSY, taking into account the leading, gluino induced contributions within the mass insertion approximation [50, 51]

$$\begin{aligned}
\delta_{\text{SUSY}}C_7^{(\prime)}(M) &= -\frac{16}{9\sqrt{2}G_F}\frac{\alpha_s\pi}{m_{\tilde{q}}^2}(\delta_{12})_{LR(RL)}\frac{m_{\tilde{g}}}{m_c}M_1(x)\,,\\
\delta_{\text{SUSY}}C_8^{(\prime)}(M) &= -\frac{1}{\sqrt{2}G_F}\frac{\alpha_s\pi}{m_{\tilde{q}}^2}(\delta_{12})_{LR(RL)}\frac{m_{\tilde{g}}}{m_c}\left(-\frac{1}{3}M_1(x) - 3M_2(x)\right)\,,
\end{aligned} \tag{4.13}$$

where $m_{\tilde{q}}$ and $m_{\tilde{g}}$ denote the masses of the squarks and the gluino, respectively, $M \sim m_{\tilde{g},\tilde{q}}$,

$$\begin{aligned}
M_1(x) &= \frac{1+4x-5x^2+4x\ln x+2x^2\ln x}{2(1-x)^4}\,, & M_1(x=1) &= \frac{1}{12}\,,\\
M_2(x) &= -x^2\frac{5-4x-x^2+2\ln x+4x\ln x}{2(1-x)^4}\,, & M_2(x=1) &= \frac{1}{12}\,,
\end{aligned} \tag{4.14}$$

and $x = m_{\tilde{g}}^2/m_{\tilde{q}}^2$. We neglected terms not subject to $m_{\tilde{g}}/m_c$-enhancement.

The mass insertions (δ_{12}) are constrained by data on the $D^0 - \bar{D}^0$ mass difference [36, 50]. In case of *i)*: $m_{\tilde{g}}^{(i)} = 1\,\text{TeV}$, $m_{\tilde{q}}^{(i)} = 2\,\text{TeV}$ and *ii)*: $m_{\tilde{g}}^{(ii)} = 2\,\text{TeV}$, $m_{\tilde{q}}^{(ii)} = 1\,\text{TeV}$, we find

$$\sqrt{\left|\text{Re}(\delta_{12}^{(i)})_{LR,RL}^2\right|} \lesssim 0.07\,, \qquad \sqrt{\left|\text{Re}(\delta_{12}^{(ii)})_{LR,RL}^2\right|} \lesssim 0.02\,, \tag{4.15}$$

JHEP08(2017)091

and $|\delta^{(i)}_{\rm SUSY} A_7^{(\prime)}| \lesssim 0.2$ and $|\delta^{(ii)}_{\rm SUSY} A_7^{(\prime)}| \lesssim 0.3$, respectively. The upper limits are similar to the model-independent constraints obtained in section 4.1. Note that, barring cancellations, constraints on the imaginary parts of δ_{12} can be about an order of magnitude stronger [52], still permitting to signal BSM CP-violation. Constraints from ϵ'/ϵ and chargino loops are model-dependent. For realistic, not too low SUSY mass parameters corresponding bounds, e.g. [53], are not stronger than those from $D - \bar{D}$ mixing. We further checked that $|\delta^{(i),(ii)}_{\rm SUSY} C^{(\prime)}_{3-6}(M)| \lesssim 10^{-5}$ is negligible. Note that $|\delta_{\rm SUSY} A_7^{(\prime)} / \delta_{\rm SUSY} A_8^{(\prime)}| \in [0.75, 5.46]$, where the lower limit is for $x \gtrsim 10$ and the upper limit for $x \lesssim 0.01$. Thus, supersymmetric models may induce $c \to u\gamma$ branching ratios and CP asymmetries above the SM predictions, and SUSY parameters are constrained by $\mathcal{B}(D^0 \to \rho^0\gamma)$. Note that additional constraints may apply once the SUSY breaking has been specified [51]. A detailed evaluation is beyond the scope of this work.

5 On $\Lambda_c \to p\gamma$

We investigate possibilities to probe the handedness of the $c \to u\gamma$ current in the decay $\Lambda_c \to p\gamma$ with polarization asymmetries, that arise once Λ_c's are produced polarized. We follow closely related works on $\Lambda_b \to \Lambda\gamma$ decays [54, 55].

The $\Lambda_c \to p\gamma$ branching ratio is not measured to date. Quite generally we assume

$$\mathcal{B}(\Lambda_c \to p\gamma) \sim \mathcal{O}(10^{-5})\,, \tag{5.1}$$

in agreement with naive expectations from $\mathcal{B}(D^0 \to \rho^0\gamma)$.[3] Note, we employ equation (5.1) only to estimate uncertainties. $\mathcal{B}(\Lambda_c \to p\gamma)$ should be determined experimentally.

The number of $\Lambda_c \to p\gamma$ events N, modulo reconstruction efficiencies, can be obtained from

$$N = N(c\bar{c})\, f(c \to \Lambda_c)\, \mathcal{B}(\Lambda_c \to p\gamma) \sim N(c\bar{c}) \cdot 10^{-6}\,, \tag{5.2}$$

where $f(c \to \Lambda_c) \simeq 0.06$ [63] is the fragmentation fraction of charm to Λ_c-baryons and $N(c\bar{c})$ the number of $c\bar{c}$ produced. At the forthcoming Belle II experiment, where $\sigma(e^+e^- \to \bar{c}c) \simeq 1.3\,\text{nb}$, $L \simeq 5\,\text{ab}^{-1}$ within a year [2], $N \sim [10^3, 10^4]$. At a future e^+e^--collider running at the Z (FCC-ee), where $N(Z) \sim 10^{12}$ within one year [19] and $\mathcal{B}(Z \to c\bar{c}) \simeq 0.12$ [36], $N \sim 10^5$. This environment suggests a measurement of the $\Lambda_c \to p\gamma$ branching ratio, the Λ_c polarization and the angular asymmetry A^γ of $\Lambda_c \to p\gamma$ decays. The latter is defined in the Λ_c rest frame by the angle between the Λ_c spin and the proton momentum, that is, the forward-backward asymmetry of the photon momentum relative to the Λ_c boost, and normalized to the width. It reads [54]

$$A^\gamma = -\frac{P_{\Lambda_c}}{2}\frac{1-|r|^2}{1+|r|^2}\,, \tag{5.3}$$

[3] Via weak annihilation $r(\Lambda_c \to p\gamma/D^0 \to \rho^0\gamma) \sim \sqrt{2}$ due to color counting, via resonances $r(\Lambda_c \to p\gamma/D^0 \to \rho^0\gamma) \sim 1$ due to the amplitude $A^{\rm III,\Lambda_c\to p\gamma}$ [56] and $r(\Lambda_c \to p\gamma/D^0 \to \rho^0\gamma) \simeq \sqrt{2} f_\perp/T \sim 1$ via SM effective and BSM Wilson coefficients. Here, the form factor $f_\perp = f_\perp^T(0) = f_\perp^{T5}(0)$ is defined as in [57] and calculated within QCD LCSR [58, 59], a covariant confined quark model [60] and a relativistic quark model [61]. Within a constituent quark model $\mathcal{B}_{\Lambda_c\to p\gamma} = 2.2 \cdot 10^{-5}$ [62] in agreement with eq. (5.1).

JHEP08(2017)091

where P_{Λ_c} denotes the (longitudinal) Λ_c polarization and $r = A_7'/A_7$. $A^\gamma \to P_{\Lambda_c}/2$ for $r \to \infty$ and $A^\gamma \to -P_{\Lambda_c}/2$ for $r \to 0$. Calculating A_7, A_7' in the SM is a difficult task and beyond the scope of our work. In the subsequent estimates of BSM sensitivity we assume that approximately $A_7^{(\prime)} \sim \delta C_7^{(\prime)}$ for large BSM effects and $A_7' \ll A_7$ in SM-like situations. A^γ is measurable in the laboratory frame for a boost $\vec{\beta} = \vec{p}_{\Lambda_c}/E_{\Lambda_c}$, where $\vec{p}_{\Lambda_c}$ denotes the Λ_c three-momentum in the laboratory frame, as

$$\langle q_\parallel \rangle_{|\vec{\beta}|} = \gamma E_\gamma^* \left(\left|\vec{\beta}\right| + \frac{2}{3} A^\gamma \right) . \tag{5.4}$$

Here, $\langle q_\parallel \rangle_{|\vec{\beta}|}$ is the average longitudinal momentum of the photon in the laboratory frame relative to the boost axis, $\gamma = 1/\sqrt{1-|\vec{\beta}|^2}$ and $E_\gamma^* = (m_{\Lambda_c}^2 - m_p^2)/(2m_{\Lambda_c}) \simeq 0.95\,\text{GeV}$ is the photon energy in the Λ_c rest frame.

The Λ_c polarization can be expressed in terms of the charm quarks' polarization P_c as [55, 64, 65]

$$\frac{P_{\Lambda_c}}{P_c} \simeq \frac{1 + A(0.07 + 0.46\omega_1)}{1 + A} \simeq 0.68 \pm 0.03\,, \tag{5.5}$$

where $A \simeq 1.1$ is extrapolated [64] from a measurement by the E791 collaboration [66] and $\omega_1 = 0.71 \pm 0.13$ is measured by the CLEO collaboration [67]. At the Z the polarization of the charm-quark $P_c^{(Z)} \simeq -0.65$ [68] and one obtains a sizable polarization

$$P_{\Lambda_c}^{(Z)} \simeq -0.44 \pm 0.02\,. \tag{5.6}$$

The polarization is negative since c-quarks from the Z are predominantly left-handed. Ultimately, its value needs to be determined experimentally, e.g., from $\Lambda_c \to \Lambda(\to p\pi) l\nu$ decays with $\mathcal{B}(\Lambda_c \to \Lambda(\to p\pi) e\nu_e) \simeq 0.023$ [36]. Note that the depolarization parameters A and ω_1 are measurable at Atlas, BaBar, Belle, CMS and LHCb [64]. The Λ_c polarization itself is measurable at Atlas, CMS and LHCb via $pp \to t(\to bW^+(\to c\bar{s}))\bar{t}(\to \bar{b}W^-(\to l^-\bar{\nu}))$ [64] and $pp \to W^- c$ [65], where $P_c^{(W^-)} \simeq -0.97$ [68].

The angular asymmetry is shown in figure 6 for P_{Λ_c} as expected at the Z, eq. (5.6). In the SM and leptoquark models $r \lesssim 0.2$, and $A^\gamma \sim -P_{\Lambda_c}/2$ and positive. The statistical uncertainty $\delta A^\gamma = \sqrt{1-(A^\gamma)^2}/\sqrt{N}$ is represented by the bands corresponding to $N = 10^3$ (orange) and $N = 10^5$ (purple). Within SUSY already for $N = 10^3$ the angular asymmetry could be observed essentially everywhere within $|A^\gamma| \lesssim |P_{\Lambda_c}|/2$, allowing to signal BSM physics. Prerequisite for an interpretation is an experimental determination of P_{Λ_c} or the depolarization fraction, if P_c is known.

Given the uncertainties present in meson decays our analysis of Λ_c's is clearly explorative, pointing out an opportunity with future polarization measurements with baryons. More work is needed to detail wrong-chirality contributions in the SM.

6 Summary

We worked out SM predictions for various $D_{(s)} \to V\gamma$ branching ratios, which are compiled in tables 1 and 2. The hybrid model predicts values up to a factor $\sim 2-3$ larger than the

JHEP08(2017)091

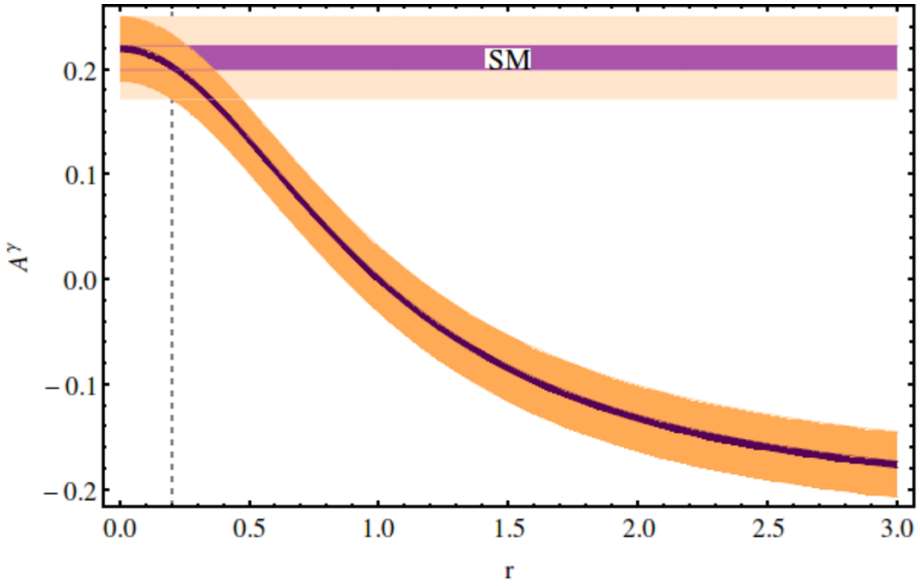

Figure 6. The angular asymmetry (5.3) of $\Lambda_c \to p\gamma$ decays as a function of $r = A_7'/A_7$ for $P_{\Lambda_c} = -0.44$. The bands represent the statistical uncertainties for $N = 10^3$ (orange) and $N = 10^5$ (purple). Within the SM and leptoquark models $r \lesssim 0.2$, indicated by the dashed vertical line, and corresponding A^γ-ranges shown by the horizontal bands. Within SUSY all values $r \lesssim \mathcal{O}(1)$ are possible.

QCD factorization based approach, the latter being dominated by contributions from weak annihilation. All three branching ratios measured so far, the ones of $D^0 \to \rho^0\gamma, D^0 \to \phi\gamma$ and $D^0 \to \bar{K}^{*0}\gamma$ are above the QCD factorization range given, suggesting, to the order we are working, a low value of the parameter $\lambda_D \lesssim 0.1\,\text{GeV}$ or low charm mass scale. One has to keep in mind, however, that poor convergence of the $1/m_c$ and α_s-expansion prohibits a sharp conclusion without further study. Decays of charged mesons with color allowed weak annihilation contribution are better suited for extracting λ_D as there is lesser chance for large cancellations, see also figure 2. The measured branching ratios are close to the top end of the ones obtained in the hybrid model. $D^0 \to \phi\gamma$ and $D^0 \to \bar{K}^{*0}\gamma$ belong to the class of those decays with no direct contribution from electromagnetic dipole operators. Corresponding decays are listed in table 2, their branching ratios have essentially no sensitivity to BSM physics unlike the CP asymmetry in $D^0 \to \phi\gamma$, cf. equations (2.26), (3.1).

The measured $D^0 \to \rho^0\gamma$ branching ratio provides a model-independent upper limit on the decay amplitudes given in eq. (4.1), which is similar to the one from $D \to \pi\mu\mu$ decays [11]. If $\mathcal{B}(D^0 \to \rho^0\gamma)$ is saturated with BSM physics or in the SM, $\mathcal{B}(D^0 \to (\rho^0/\omega)\gamma)$ are very close to each other. For intermediate scenarios the two branching ratios can differ by orders of magnitude [7], and indicate BSM physics.

CP asymmetries in $c \to u\gamma$ transitions constitute SM null tests. We find $A_{CP}^{\text{SM}} \lesssim \text{few} \cdot 10^{-3}$ for $D^0 \to \rho^0\gamma$, see figure 3, and similar for other radiative rare charm decays. Among the modes in tables 1 A_{CP} is measured only in $D^0 \to \rho^0\gamma$ decays, eq. (1.1), consistent with zero and the SM. Uncertainties on A_{CP} are presently too large to provide phenomenologically useful constraints. However, CP-violating BSM can induce significant

JHEP08(2017)091

CP asymmetries at the level of $\sim \mathcal{O}(0.1)$, and as demonstrated in figure 4, already a factor four reduction of statistical uncertainty (with central values kept) shows that constraints can be improved significantly.

We worked out implications for two BSM models, SUSY and leptoquark ones. We find that SUSY can saturate the measured $D^0 \to \rho^0\gamma$ branching ratio and CP asymmetry while leptoquark models can't. In the latter CP asymmetries $\lesssim 10\%$ are possible. The largest effects stem from models with vector leptoquarks $\tilde{V}_1$ followed by $\tilde{V}_2$ and scalars S_1, S_2 with couplings to taus.

If Λ_c-baryons are produced polarized, such as at the Z, angular asymmetries in $\Lambda_c \to p\gamma$ can probe chirality-flipped contributions, see figure 6. Within SUSY A^γ can be very different from its SM-value, including having its sign flipped. Prerequisite for an interpretation of A^γ is a measurement of the Λ_c polarization, however, irrespective of its precise value, in the SM A^γ is expected to be positive at the Z. The branching ratio of $\Lambda_c \to p\gamma$ may be investigated at Belle II [2], the depolarization fraction at the LHC [65], and at the FCC-ee [19] all of this including A^γ.

We analyzed radiative rare charm decays in the SM and beyond with presently available technologies. Both the heavy quark and the hybrid framework share qualitatively similar phenomenology. The reason is the dominance of weak annihilation and corresponding color and CKM factors. A closer look exhibits numerical differences between the two frameworks for branching ratios and CP asymmetries, detailed in section 3. Despite the considerable uncertainties we demonstrated that existing charm data are already informative on BSM physics. Future measurements can improve theoretical frameworks and allow to check for patterns. Given the unique window into flavor in the up-sector that is provided by $|\Delta C| = |\Delta U| = 1$ processes, further efforts are worthwhile and necessary. Largest sources of parametric uncertainty within the SM are the μ_c-scale dependence and λ_D in the heavy quark approach and $a_{1,2}$ and the form factor $A_1(q^2)$ in the hybrid model. For a BSM interpretation in scenarios with enhanced dipole operators improved knowledge of $D \to V$ tensor form factors at $q^2 = 0$ is desirable.

Acknowledgments

We thank Jernej Kamenik, Kamila Kowalska, Stephane Monteil, Stefan Schacht and Alan Schwartz for useful discussions. This work has been supported in part by the DFG Research Unit FOR 1873 "Quark Flavour Physics and Effective Field Theories".

A Parameters

The couplings, the ($\overline{\text{MS}}$) masses and the widths are taken from the PDG [36], with the renormalization scale running as in [69]. The values of the CKM matrix elements are taken from the UTfit collaboration [70]. The decay constants given by the FLAG read [71]

$$\begin{aligned} f_{D_s} &= (0.24883 \pm 0.00127)\,\text{GeV}\,, & f_D &= (0.21215 \pm 0.00145)\,\text{GeV}\,, \\ f_K &= (0.1556 \pm 0.0004)\,\text{GeV}\,, & f_\pi &= (0.1302 \pm 0.0014)\,\text{GeV} \end{aligned} \tag{A.1}$$

and [33, 72] (and references therein)

$$
\begin{aligned}
f_\phi &= (0.233 \pm 0.004)\,\text{GeV}\,, & & & (A.2)\\
f_{K^*} &= (0.204 \pm 0.007)\,\text{GeV}\,, & & f_{K^*}^\perp = (0.163 \pm 0.008)\,\text{GeV}\,,\\
f_\rho &= (0.213 \pm 0.005)\,\text{GeV}\,, & f_{\rho^0}^{(d)} = (0.2097 \pm 0.0003)\,\text{GeV}\,, & f_\rho^\perp = (0.160 \pm 0.011)\,\text{GeV}\,,\\
f_\omega &= (0.197 \pm 0.008)\,\text{GeV}\,, & f_\omega^{(d)} = (0.2013 \pm 0.0008)\,\text{GeV}\,, & f_\omega^\perp = (0.139 \pm 0.018)\,\text{GeV}
\end{aligned}
$$

at $\mu = 1\,\text{GeV}$ for the transverse decay constants.

The Gegenbauer moments read [33] (and references therein)

$$
\begin{aligned}
a_1^{\rho\perp} &= 0\,, & a_2^{\rho\perp} &= 0.14 \pm 0.06\,,\\
a_1^{\omega\perp} &= 0\,, & a_2^{\omega\perp} &= 0.14 \pm 0.12\,,\\
a_1^{K^*\perp} &= -0.04 \pm 0.03\,, & a_2^{K^*\perp} &= 0.10 \pm 0.08
\end{aligned}
\qquad (A.3)
$$

at $\mu = 1\,\text{GeV}$, where the sign of $a_1^{K^*\perp}$ is due to $K^{*+} = (u\bar{s})$ [29].

B $D \to V$ form factors

We define the $D \to V$ form factors as usual

$$
\begin{aligned}
\langle V(p_V,\epsilon^\nu)|\bar{u}\gamma_\mu(1-\gamma_5)c|D(p_D)\rangle &= -2\epsilon_{\mu\nu_1\nu_2\nu_3}(\epsilon^*)^{\nu_1}p_D^{\nu_2}q^{\nu_3}\frac{V(q^2)}{m_D+m_V} \qquad (B.1)\\
&\quad + i\left(q_\mu\frac{\epsilon^*\cdot q}{q^2} - \epsilon_\mu^*\right)(m_D+m_V)A_1(q^2)\\
&\quad - i\left(q_\mu\frac{m_D^2-m_V^2}{q^2} - (p_D+p_V)_\mu\right)\frac{\epsilon^*\cdot q}{m_D+m_V}A_2(q^2)\\
&\quad - iq_\mu(\epsilon^*\cdot q)\frac{2m_V}{q^2}A_0(q^2)\,,\\
\langle V(p_V,\epsilon^\nu)|\bar{u}\sigma_{\mu\nu}q^\nu(1+\gamma_5)c|D(p_D)\rangle &= -i2\epsilon_{\mu\nu_1\nu_2\nu_3}(\epsilon^*)^{\nu_1}p_D^{\nu_2}q^{\nu_3}T_1(q^2)\\
&\quad - \left((p_D+p_V)_\mu(\epsilon^*\cdot q) - \epsilon_\mu^*\left(m_D^2-m_V^2\right)\right)T_2(q^2)\\
&\quad + \left(q_\mu - (p_D+p_V)_\mu\frac{q^2}{m_D^2-m_V^2}\right)(\epsilon^*\cdot q)T_3(q^2)\,,
\end{aligned}
$$

where $\epsilon_{0123} = 1$ and $q_\mu = (p_D - p_V)_\mu$. In our analysis we need $V(0), T_1(0)$ and $A_1(q^2)$.

The $D \to \rho$ form factors have been measured by the CLEO collaboration [73] as

$$
V(0) = 0.84^{+0.10}_{-0.11}\,, \quad A_1(0) = 0.56^{+0.02}_{-0.03}\,, \quad V(0)/A_1(0) = 1.48 \pm 0.16\,, \qquad (B.2)
$$

where statistical and systematic uncertainties are added in quadrature, consistent with lattice computations [74] (and references therein)

$$
V(0) = 1.1 \pm 0.2\ (0.71^{+0.10}_{-0.12})\,, \quad A_1(0) = 0.65 \pm 0.07\ (0.60 \pm 0.06)\,. \qquad (B.3)
$$

Here, given in parenthesis are the preliminary computations of [75] with doubled uncertainties to account for systematic uncertainties. The $D \to \omega$ form factors have been measured

JHEP08(2017)091

by the BESIII collaboration [76] as (statistical and systematic uncertainties are added in quadrature)

$$V(0)/A_1(0) = 1.24 \pm 0.11\,, \tag{B.4}$$

consistent with the values for $D \to \rho$, equation (B.2).

The (axial-)vector form factors have been obtained from QCD LCSR [77]

$$\begin{aligned} &V(0) = 0.80 \pm 0.04\,, && A_1(0) = 0.60^{+0.04}_{-0.03}\,, && (D \to \rho)\\ &V(0) = 0.74^{+0.04}_{-0.03}\,, && A_1(0) = 0.56 \pm 0.03\,, && (D \to \omega)\\ &V(0) = 0.77 \pm 0.05\,, && A_1(0) = 0.59 \pm 0.04 && (D_s \to K^*) \end{aligned} \tag{B.5}$$

and

$$A_1^{(D\to K^*)}(0) = 0.57 \pm 0.02\,, \quad A_1^{(D_s\to\phi)}(0) = 0.57 \pm 0.05\,, \tag{B.6}$$

where we rounded for easier comparison. The constituent quark model (CQM) [78] and the covariant light-front quark model (CLFQM) [79] provide q^2-shapes for the form factors. Note that we do not employ the form factors of [80] within chiral theory as the $D \to \rho, \omega$ form factors at $q^2 = 0$ and the $D \to \pi$ form factors differ from measurements/computations.

In the numerical analysis we employ the following form factor values

$$\begin{aligned} &T_1(0) = 0.7(1 \pm 0.20)\,, && V(0) = 0.9(1 \pm 0.25)\,, && (D \to (\rho,\omega)\gamma)\\ &T_1(0) = 0.7(1 \pm 0.25)\,, && V(0) = 0.9(1 \pm 0.30)\,, && (D_s \to K^*\gamma) \end{aligned} \tag{B.7}$$

$$A_1^{(c\to u)}(q^2) = \frac{0.6}{1 - 0.5\,q^2/m_D^2}(1 \pm 0.15)\,, \quad A_1^{(D\to K^*, D_s\to\phi)}(q^2) = \frac{0.6}{1 - 0.5\,q^2/m_D^2}(1 \pm 0.20)\,,$$

where uncertainties are given in parenthesis. These ranges are consistent with eqs. (B.2)–(B.6), the CQM and the CLFQM as well as the large energy relations [81]. $A_1(q^2)$ is shown in figure 7.

C $D \to V\gamma$ amplitudes in the hybrid approach

We write the resonance-induced contributions to $D \to V\gamma$ amplitudes using [5, 6] and [82] as

$$A_{\rm PC/PV} = \sqrt{\alpha_e 2\pi} G_F V_{cq}^* V_{uq'} \left(A^{\rm I}_{\rm PC/PV} + A^{\rm II}_{\rm PC/PV} + A^{\rm III}_{\rm PC/PV} \right) . \tag{C.1}$$

For each $D \to V\gamma$ transition, the CKM factor $V_{cq}^* V_{uq'}$ can be inferred from the corresponding weak annihilation contribution, eqs. (2.14) and (2.23). The amplitudes $A^{\rm III}_{\rm PC/PV}$ originate from the long-distance penguin estimated with VMD. They contain terms with different CKM factors, allowing for CP violation. We adjusted the relative sign between the VMD contributions from ρ, ω and ϕ to recover $A^{\rm III}_{\rm PC/PV} = 0$ in the SU(3)-limit. For the weak annihilation modes $A^{\rm III}_{\rm PC/PV} = 0$.

For $V = V^0 \in \{\rho^0, \omega\}$ the $D^0 \to V\gamma$ amplitudes read

$$\begin{aligned} |A^{{\rm I},V^0}_{\rm PC}| = &- \frac{m_{D^{*0}}^{7/2}\left(m_{D^{*0}}^2 - (m_{D^0} + m_{\pi^0})^2\right)^{3/4}\left(m_{D^{*0}}^2 - (m_{D^0} - m_{\pi^0})^2\right)^{3/4} m_{V^0}}{\sqrt{2\pi\alpha_e} m_{D^0}^{3/2}(m_{D^{*0}}^2 - m_{D^0}^2)^{3/2}(m_{D^{*0}} + m_{D^0} - m_{\pi^0})(m_{D^{*0}}^2 - m_{V^0}^2)}\\ &\times a_2 f_{V^0}\sqrt{\frac{\Gamma(D^{*0}\to D^0\gamma)}{\Gamma(D^{*0}\to D^0\pi^0)}} f_+(0), \end{aligned}$$

JHEP08(2017)091

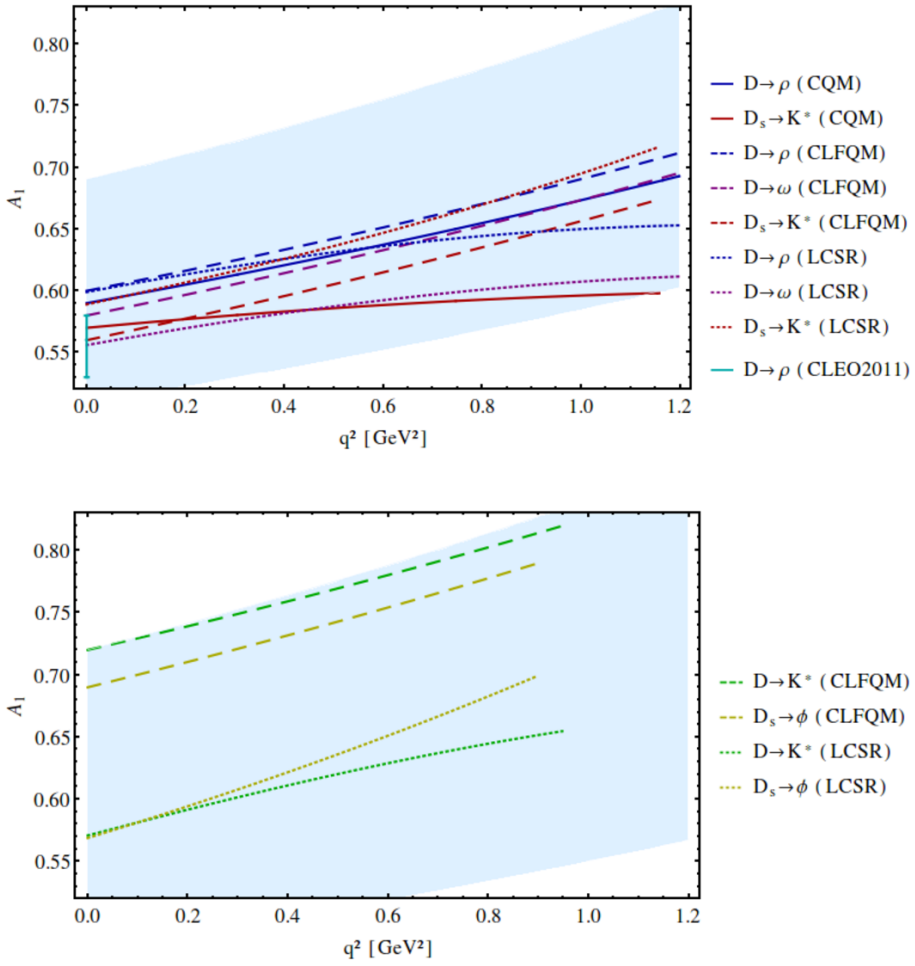

Figure 7. The form factor $A_1(q^2)$ from the CQM [78] (solid curves), the CLFQM [79] (dashed curves) and LCSR [77] (dotted curves). The blue, purple, red, green and yellow curves are for $D \to \rho$, $D \to \omega$, $D_s \to K^*$, $D \to K^*$ and $D_s \to \phi$, respectively. The curves are shown in the kinematically allowed regions only. The (cyan) error bar depicts the $D \to \rho$ measurement [73]. The light blue bands represent the values employed in the numerical analysis, eq. (B.7).

$$
\begin{aligned}
|A_{\rm PC}^{{\rm II},V^0}| &= \frac{2\sqrt{3}m_{D^0}^2}{\sqrt{\alpha_e}(m_{D^0}^2-m_{\pi^0}^2)} \\
&\quad \times a_2 f_D f_\pi \left(\sqrt{\Gamma(\rho^0\to\pi^0\gamma)}\frac{m_\rho^{3/2}}{(m_\rho^2-m_{\pi^0}^2)^{3/2}} - \sqrt{\Gamma(\omega\to\pi^0\gamma)}\frac{m_\omega^{3/2}}{(m_\omega^2-m_{\pi^0}^2)^{3/2}} \right), \\
|A_{\rm PC}^{{\rm III},V^0}| &= \frac{1}{m_{D^0}+m_{V^0}} a_2 \left(-f_\rho^2 + \frac{1}{3}f_\omega^2 - \frac{V_{cs}^* V_{us}}{V_{cd}^* V_{ud}}\frac{2}{3}f_\phi^2 \right) V^{V^0}(0), \\
|A_{\rm PV}^{{\rm I},V^0}| &= 0, \\
|A_{\rm PV}^{{\rm II},V^0}| &= -\frac{1}{\sqrt{2}(m_{D^0}^2-m_{V^0}^2)} a_2 f_\rho \left(f_\rho A_1^\rho(m_{V^0}^2)(m_{D^0}+m_\rho) + f_\omega A_1^\omega(m_{V^0}^2)\frac{(m_{D^0}+m_\omega)m_\rho}{3m_\omega} \right), \\
|A_{\rm PV}^{{\rm III},V^0}| &= \frac{1}{m_{D^0}-m_{V^0}} a_2 \left(-f_\rho^2 + \frac{1}{3}f_\omega^2 - \frac{V_{cs}^* V_{us}}{V_{cd}^* V_{ud}}\frac{2}{3}f_\phi^2 \right) A_1^{V^0}(0)
\end{aligned}
\tag{C.2}
$$

JHEP08(2017)091

and for $D^+ \to \rho^+\gamma$

$$
\begin{aligned}
|A_{\rm PC}^{{\rm I},\rho^+}| &= \frac{m_{D^{*+}}^{7/2}\left(m_{D^{*+}}^2-(m_{D^+}+m_{\pi^0})^2\right)^{3/4}\left(m_{D^{*+}}^2-(m_{D^+}-m_{\pi^0})^2\right)^{3/4}m_\rho}{\sqrt{\pi\alpha_e}m_{D^+}^{3/2}(m_{D^{*+}}^2-m_{D^+}^2)^{3/2}(m_{D^{*+}}+m_{D^+}-m_{\pi^+})(m_{D^{*+}}^2-m_\rho^2)} \\
&\quad\times a_1 f_\rho\sqrt{\frac{\Gamma(D^{*+}\to D^+\gamma)}{\Gamma(D^{*+}\to D^+\pi^0)}}f_+(0)\,, \\
|A_{\rm PC}^{{\rm II},\rho^+}| &= \frac{2\sqrt{6}m_{D^+}^2m_\rho^{3/2}}{\sqrt{\alpha_e}(m_{D^+}^2-m_{\pi^+}^2)(m_\rho^2-m_{\pi^+}^2)^{3/2}}a_1 f_D f_\pi\sqrt{\Gamma(\rho^+\to\pi^+\gamma)}\,, \\
|A_{\rm PC}^{{\rm III},\rho^+}| &= \frac{1}{m_{D^+}+m_\rho}a_2\left(-f_\rho^2+\frac{1}{3}f_\omega^2-\frac{V_{cs}^*V_{us}}{V_{cd}^*V_{ud}}\frac{2}{3}f_\phi^2\right)V^\rho(0)\,, \\
|A_{\rm PV}^{{\rm I},\rho^+}| &= \frac{2m_\rho}{m_{D^+}^2-m_\rho^2}a_1 f_D f_\rho\,, \\
|A_{\rm PV}^{{\rm II},\rho^+}| &= \frac{1}{m_{D^+}^2-m_\rho^2}a_1 f_\rho\left(f_\rho A_1^\rho(m_\rho^2)(m_{D^+}+m_\rho)-f_\omega A_1^\omega(m_\rho^2)\frac{(m_{D^+}+m_\omega)m_\rho}{3m_\omega}\right)\,, \\
|A_{\rm PV}^{{\rm III},\rho^+}| &= \frac{1}{m_{D^+}-m_\rho}a_2\left(-f_\rho^2+\frac{1}{3}f_\omega^2-\frac{V_{cs}^*V_{us}}{V_{cd}^*V_{ud}}\frac{2}{3}f_\phi^2\right)A_1^\rho(0)\,,
\end{aligned}
\tag{C.3}
$$

where $a_{1,2}$ are given in section 3 and $f_+(0) = (0.1426 \pm 0.0019)/|V_{cd}|$ [42], where statistical and systematic uncertainties are added in quadrature. For $D_s \to K^{*+}\gamma$ decays

$$
\begin{aligned}
|A_{\rm PC}^{{\rm I},K^{*+}}| &= \frac{4m_{D_s^*}^{3/2}m_{K^{*+}}}{m_{D_s}^{1/2}(m_{D_s^*}^2-m_{K^{*+}}^2)}a_1 f_{D_s}f_{K^*}\left|\lambda'+\lambda\tilde{g}_V\frac{-f_\phi}{3\sqrt{2}m_\phi}\right|\,, \\
|A_{\rm PC}^{{\rm II},K^{*+}}| &= \frac{2\sqrt{6}m_{D_s}^2m_{K^{*+}}^{3/2}}{\sqrt{\alpha_e}(m_{D_s}^2-m_{K^+}^2)(m_{K^{*+}}^2-m_{K^+}^2)^{3/2}}a_1 f_{D_s}f_K\sqrt{\Gamma(K^{*+}\to K^+\gamma)}\,, \\
|A_{\rm PC}^{{\rm III},K^{*+}}| &= \frac{1}{m_{D_s}+m_{K^{*+}}}a_2\left(-\frac{V_{cd}^*V_{ud}}{V_{cs}^*V_{us}}\left(-f_\rho^2+\frac{1}{3}f_\omega^2\right)+\frac{2}{3}f_\phi^2\right)V^{K^*}(0)\,, \\
|A_{\rm PV}^{{\rm I},K^{*+}}| &= \frac{2m_{K^{*+}}}{m_{D_s}^2-m_{K^{*+}}^2}a_1 f_{D_s}f_{K^*}\,, \\
|A_{\rm PV}^{{\rm II},K^{*+}}| &= \frac{2(m_{D_s}+m_\phi)m_{K^{*+}}}{3m_\phi(m_{D_s}^2-m_{K^{*+}}^2)}a_1 f_{K^*}f_\phi A_1^{(D_s\to\phi)}(m_{K^{*+}}^2)\,, \\
|A_{\rm PV}^{{\rm III},K^{*+}}| &= \frac{1}{m_{D_s}-m_{K^{*+}}}a_2\left(-\frac{V_{cd}^*V_{ud}}{V_{cs}^*V_{us}}\left(-f_\rho^2+\frac{1}{3}f_\omega^2\right)+\frac{2}{3}f_\phi^2\right)A_1^{K^*}(0)\,.
\end{aligned}
\tag{C.4}
$$

As the approximation of [5, 6] is not applicable for $\mathcal{B}(D_s^* \to D_s\pi^0)$ as a normalization mode due to isospin breaking [83] and $\Gamma_{D_s^*}$ is not measured, λ' and $\lambda\tilde{g}_V$ in $A_{\rm PC}^{{\rm I},K^{*+}}$ are related to

$$
\begin{aligned}
\left|\lambda'+\lambda\tilde{g}_V\left(\pm\frac{f_\rho}{2\sqrt{2}m_\rho}+\frac{f_\omega}{6\sqrt{2}m_\omega}\right)\right| &= \frac{m_{D^*}^2\left(m_{D^*}^2-(m_D+m_{\pi^0})^2\right)^{3/4}\left(m_{D^*}^2-(m_D-m_{\pi^0})^2\right)^{3/4}}{4\sqrt{\pi\alpha_e}m_D(m_{D^*}^2-m_D^2)^{3/2}(m_{D^*}+m_D-m_{\pi^{0/+}})} \\
&\quad\times\frac{f_+(0)}{f_D}\sqrt{\frac{\Gamma(D^{*0/+}\to D^{0/+}\gamma)}{\Gamma(D^{*0/+}\to D^{0/+}\pi^0)}}
\end{aligned}
\tag{C.5}
$$

JHEP08(2017)091

and the ambiguity is fixed by means of the form factor V [82]

$$\lambda\tilde{g}_V = \frac{V^V(0)}{f_D}\frac{\sqrt{2}m_{D^*}^2}{(m_D+m_V)(m_{D^*}+m_D-m_V)}\,. \tag{C.6}$$

Furthermore,

$$\begin{aligned}
|A_{\rm PC}^{{\rm I},D^0\to\phi\gamma}| &= -\frac{m_{D^{*0}}^{7/2}\left(m_{D^{*0}}^2-(m_{D^0}+m_{\pi^0})^2\right)^{3/4}\left(m_{D^{*0}}^2-(m_{D^0}-m_{\pi^0})^2\right)^{3/4}m_\phi}{\sqrt{\pi\alpha_e}m_{D^0}^{3/2}(m_{D^{*0}}^2-m_{D^0}^2)^{3/2}(m_{D^{*0}}+m_{D^0}-m_{\pi^0})(m_{D^{*0}}^2-m_\phi^2)} \\
&\quad\times a_2 f_\phi\sqrt{\frac{\Gamma(D^{*0}\to D^0\gamma)}{\Gamma(D^{*0}\to D^0\pi^0)}}f_+(0)\,, \\
|A_{\rm PC}^{{\rm II},D^0\to\phi\gamma}| &= -\frac{8m_{D^0}^2}{3(m_{D^0}^2-m_{K^0}^2)m_\phi}a_2 f_D f_\phi|C_{VV\Pi}|\,, \\
|A_{\rm PV}^{{\rm I},D^0\to\phi\gamma}| &= 0\,, \\
|A_{\rm PV}^{{\rm II},D^0\to\phi\gamma}| &= -\frac{m_\phi}{m_{D^0}^2-m_\phi^2}a_2 f_\phi\left(f_\rho A_1^\rho(m_\phi^2)\frac{m_{D^0}+m_\rho}{m_\rho}+f_\omega A_1^\omega(m_\phi^2)\frac{m_{D^0}+m_\omega}{3m_\omega}\right)\,,
\end{aligned} \tag{C.7}$$

where

$$|C_{VV\Pi}| = \frac{\sqrt{6}m_{K^{*0/+}}^{3/2}}{\sqrt{\alpha_e}(m_{K^{*0/+}}^2-m_{K^{0/+}}^2)^{3/2}}\frac{f_K}{\left|\mp\frac{f_\rho}{m_\rho}+\frac{f_\omega}{3m_\omega}-\frac{2f_\phi}{3m_\phi}\right|}\sqrt{\Gamma(K^{*0/+}\to K^{0/+}\gamma)} \tag{C.8}$$

yields $|C_{VV\Pi}|\simeq 0.3$,

$$\begin{aligned}
|A_{\rm PC}^{{\rm I},D^0\to\bar{K}^{*0}\gamma}| &= -\frac{m_{D^{*0}}^{7/2}\left(m_{D^{*0}}^2-(m_{D^0}+m_{\pi^0})^2\right)^{3/4}\left(m_{D^{*0}}^2-(m_{D^0}-m_{\pi^0})^2\right)^{3/4}m_{K^{*0}}}{\sqrt{\pi\alpha_e}m_{D^0}^{3/2}(m_{D^{*0}}^2-m_{D^0}^2)^{3/2}(m_{D^{*0}}+m_{D^0}-m_{\pi^0})(m_{D^{*0}}^2-m_{K^{*0}}^2)} \\
&\quad\times a_2 f_{K^*}\sqrt{\frac{\Gamma(D^{*0}\to D^0\gamma)}{\Gamma(D^{*0}\to D^0\pi^0)}}f_+(0), \\
|A_{\rm PC}^{{\rm II},D^0\to\bar{K}^{*0}\gamma}| &= -\frac{2\sqrt{6}m_{D^0}^2m_{K^{*0}}^{3/2}}{\sqrt{\alpha_e}(m_{D^0}^2-m_{K^0}^2)(m_{K^{*0}}^2-m_{K^0}^2)^{3/2}}a_2 f_D f_K\sqrt{\Gamma(K^{*0}\to K^0\gamma)}, \\
|A_{\rm PV}^{{\rm I},D^0\to\bar{K}^{*0}\gamma}| &= 0, \\
|A_{\rm PV}^{{\rm II},D^0\to\bar{K}^{*0}\gamma}| &= -\frac{m_{K^{*0}}}{m_{D^0}^2-m_{K^{*0}}^2}a_2 f_{K^*}\left(f_\rho A_1^\rho(m_{K^{*0}}^2)\frac{m_{D^0}+m_\rho}{m_\rho}+f_\omega A_1^\omega(m_{K^{*0}}^2)\frac{m_{D^0}+m_\omega}{3m_\omega}\right), \\
|A_{\rm PC,PV}^{{\rm I,II},D^0\to K^{*0}\gamma}| &= |V_{cd}^*V_{us}/(V_{cs}^*V_{ud})||A_{\rm PC,PV}^{{\rm I,II},D^0\to\bar{K}^{*0}\gamma}|, \\
|A_{\rm PC}^{{\rm I},D^+\to K^{*+}\gamma}| &= \frac{m_{D^{*+}}^{7/2}\left(m_{D^{*+}}^2-(m_{D^+}+m_{\pi^0})^2\right)^{3/4}\left(m_{D^{*+}}^2-(m_{D^+}-m_{\pi^0})^2\right)^{3/4}m_{K^{*+}}}{\sqrt{\pi\alpha_e}m_{D^+}^{3/2}(m_{D^{*+}}^2-m_{D^+}^2)^{3/2}(m_{D^{*+}}+m_{D^+}-m_{\pi^+})(m_{D^{*+}}^2-m_{K^{*+}}^2)} \\
&\quad\times a_1 f_{K^*}\sqrt{\frac{\Gamma(D^{*+}\to D^+\gamma)}{\Gamma(D^{*+}\to D^+\pi^0)}}f_+(0), \\
|A_{\rm PC}^{{\rm II},D^+\to K^{*+}\gamma}| &= \frac{2\sqrt{6}m_{D^+}^2m_{K^{*+}}^{3/2}}{\sqrt{\alpha_e}(m_{D^+}^2-m_{K^+}^2)(m_{K^{*+}}^2-m_{K^+}^2)^{3/2}}a_1 f_D f_K\sqrt{\Gamma(K^*\to K^+\gamma)}, \\
|A_{\rm PV}^{{\rm I},D^+\to K^{*+}\gamma}| &= \frac{2m_{K^{*+}}}{m_{D^+}^2-m_{K^{*+}}^2}a_1 f_D f_{K^*},
\end{aligned} \tag{C.9, C.10}$$

JHEP08(2017)091

$$|A_{\rm PV}^{{\rm II},D^+\to K^{*+}\gamma}|=\frac{m_{K^{*+}}}{m_{D^+}^2-m_{K^{*+}}^2}a_1 f_{K^*}\left(f_\rho A_1^\rho(m_{K^{*+}}^2)\frac{m_{D^+}+m_\rho}{m_\rho}-f_\omega A_1^{(D_s\to K^*)}(m_{K^{*+}}^2)\frac{m_{D^+}+m_\omega}{3m_\omega}\right)$$

and

$$\begin{aligned}
|A_{\rm PC}^{{\rm I},D_s\to\rho^+\gamma}| &= \frac{4m_{D_s^*}^{3/2}m_\rho}{m_{D_s}^{1/2}(m_{D_s^*}^2-m_\rho^2)}a_1 f_{D_s}f_\rho\left|\lambda'+\lambda\tilde{g}_V\frac{-f_\phi}{3\sqrt{2}m_\phi}\right|,\\
|A_{\rm PC}^{{\rm II},D_s\to\rho^+\gamma}| &= \frac{2\sqrt{6}m_{D_s}^2m_\rho^{3/2}}{\sqrt{\alpha_e}(m_{D_s}^2-m_{\pi^+}^2)(m_\rho^2-m_{\pi^+}^2)^{3/2}}a_1 f_{D_s}f_\pi\sqrt{\Gamma(\rho^+\to\pi^+\gamma)},\\
|A_{\rm PV}^{{\rm I},D_s\to\rho^+\gamma}| &= \frac{2m_\rho}{m_{D_s}^2-m_\rho^2}a_1 f_{D_s}f_\rho,\\
|A_{\rm PV}^{{\rm II},D_s\to\rho^+\gamma}| &= \frac{2(m_{D_s}+m_\phi)m_\rho}{3m_\phi(m_{D_s}^2-m_\rho^2)}a_1 f_\rho f_\phi A_1^{(D_s\to\phi)}(m_{K^{*+}}^2).
\end{aligned}\tag{C.11}$$

D $C_7^{\rm eff}$ from $\langle Q_{3-6}\rangle$ at two-loop QCD

We obtain contributions to $C_7^{\rm eff}$ from the two-loop QCD matrix elements of Q_{3-6} from [84]

$$C_7^{\rm eff}\big|_{\langle Q_{3-6}\rangle}(\mu_c)=(V_{cd}^*V_{ud}+V_{cs}^*V_{us})\frac{\alpha_s}{4\pi}\sum_{i=3}^{6}\left(r_i-\frac{\gamma_{i7}^{(1)\rm eff}}{2}\ln\frac{\mu_c^2}{m_c^2}\right)C_i,\tag{D.1}$$

where

$$\gamma_{37}^{(1)\rm eff}=-\frac{128}{81},\quad \gamma_{47}^{(1)\rm eff}=\frac{592}{243},\quad \gamma_{57}^{(1)\rm eff}=\frac{12928}{81},\quad \gamma_{67}^{(1)\rm eff}=\frac{40288}{243},\tag{D.2}$$

$$\begin{aligned}
r_3 &= -\frac{4784}{243}-\frac{16\pi}{3\sqrt{3}}-\frac{64}{9}X_b+2a(1)-4b(1)-\frac{112}{81}i\pi,\\
r_4 &= \frac{1270}{729}+\frac{8\pi}{9\sqrt{3}}+\frac{32}{27}X_b-\frac{1}{3}a(1)-\frac{10}{3}b(1)-4b(m_s^2/m_c^2)+\frac{248}{243}i\pi,\\
r_5 &= -\frac{113360}{243}-\frac{64\pi}{3\sqrt{3}}-\frac{256}{9}X_b+32a(1)-64b(1)-\frac{1792}{81}i\pi,\\
r_6 &= -\frac{60980}{729}+\frac{32\pi}{9\sqrt{3}}+\frac{128}{27}X_b+\frac{20}{3}a(1)-\frac{88}{3}b(1)+6a(m_s^2/m_c^2)-40b(m_s^2/m_c^2)+\frac{1520}{243}i\pi,
\end{aligned}\tag{D.3}$$

where we use $m_{u,d}=0$,

$$\begin{aligned}
a(\rho)=\frac{16}{9}\Bigg(&\left(\frac{5}{2}-\frac{1}{3}\pi^2-3\zeta_3+\left(\frac{5}{2}-\frac{3}{4}\pi^2\right)\ln\rho+\frac{1}{4}\ln^2\rho+\frac{1}{12}\ln^3\rho\right)\rho\\
&+\left(\frac{7}{4}+\frac{2}{3}\pi^2-\frac{1}{2}\pi^2\ln\rho-\frac{1}{4}\ln^2\rho+\frac{1}{12}\ln^3\rho\right)\rho^2+\left(-\frac{7}{6}-\frac{1}{4}\pi^2+2\ln\rho-\frac{3}{4}\ln^2\rho\right)\rho^3\\
&+\left(\frac{457}{216}-\frac{5}{18}\pi^2-\frac{1}{72}\ln\rho-\frac{5}{6}\ln^2\rho\right)\rho^4+\left(\frac{35101}{8640}-\frac{35}{72}\pi^2-\frac{185}{144}\ln\rho-\frac{35}{24}\ln^2\rho\right)\rho^5\\
&+\left(\frac{67801}{8000}-\frac{21}{20}\pi^2-\frac{3303}{800}\ln\rho-\frac{63}{20}\ln^2\rho\right)\rho^6\\
&+i\pi\left(\left(2-\frac{1}{6}\pi^2+\frac{1}{2}\ln\rho+\frac{1}{2}\ln^2\rho\right)\rho+\left(\frac{1}{2}-\frac{1}{6}\pi^2-\ln\rho+\frac{1}{2}\ln^2\rho\right)\rho^2+\rho^3+\frac{5}{9}\rho^4+\frac{49}{72}\rho^5+\frac{231}{200}\rho^6\right)\Bigg)\\
&+\mathcal{O}\left(\rho^7\ln^2\rho\right),
\end{aligned}$$

JHEP08(2017)091

$$
\begin{aligned}
b(\rho) = -\frac{8}{9}\Bigg(&\left(-3+\frac{1}{6}\pi^2-\ln\rho\right)\rho-\frac{2}{3}\pi^2\rho^{3/2}+\left(\frac{1}{2}+\pi^2-2\ln\rho-\frac{1}{2}\ln^2\rho\right)\rho^2\\
&+\left(-\frac{25}{12}-\frac{1}{9}\pi^2-\frac{19}{18}\ln\rho+2\ln^2\rho\right)\rho^3+\left(-\frac{1376}{225}+\frac{137}{30}\ln\rho+2\ln^2\rho+\frac{2}{3}\pi^2\right)\rho^4\\
&+\left(-\frac{131317}{11760}+\frac{887}{84}\ln\rho+5\ln^2\rho+\frac{5}{3}\pi^2\right)\rho^5+\left(-\frac{2807617}{97200}+\frac{16597}{540}\ln\rho+14\ln^2\rho+\frac{14}{3}\pi^2\right)\rho^6\\
&+i\pi\left(-\rho+(1-2\ln\rho)\rho^2+\left(-\frac{10}{9}+\frac{4}{3}\ln\rho\right)\rho^3+\rho^4+\frac{2}{3}\rho^5+\frac{7}{9}\rho^6\right)\Bigg)\\
&+\mathcal{O}\left(\rho^7\ln^2\rho\right)
\end{aligned}
\tag{D.4}
$$

and

$$
a(1) \simeq 4.0859 + \frac{4}{9}i\pi\,, \qquad b(1) \simeq 0.0316 + \frac{4}{81}i\pi\,, \qquad X_b \simeq -0.1684\,. \tag{D.5}
$$

References

[1] J.L. Hewett et al., *The discovery potential of a super B factory*, hep-ph/0503261 [INSPIRE].

[2] T. Aushev et al., *Physics at super B factory*, arXiv:1002.5012 [INSPIRE].

[3] C. Greub, T. Hurth, M. Misiak and D. Wyler, *The $c \to u\gamma$ contribution to weak radiative charm decay*, *Phys. Lett.* **B 382** (1996) 415 [hep-ph/9603417] [INSPIRE].

[4] G. Isidori and J.F. Kamenik, *Shedding light on CP-violation in the charm system via $D \to V\gamma$ decays*, *Phys. Rev. Lett.* **109** (2012) 171801 [arXiv:1205.3164] [INSPIRE].

[5] S. Fajfer and P. Singer, *Long distance $c \to u\gamma$ effects in weak radiative decays of D mesons*, *Phys. Rev.* **D 56** (1997) 4302 [hep-ph/9705327] [INSPIRE].

[6] S. Fajfer, S. Prelovsek and P. Singer, *Long distance contributions in $D \to V\gamma$ decays*, *Eur. Phys. J.* **C 6** (1999) 471 [hep-ph/9801279] [INSPIRE].

[7] S. Fajfer, S. Prelovsek, P. Singer and D. Wyler, *A possible arena for searching new physics: the $\Gamma(D^0 \to \rho^0\gamma)/\Gamma(D^0 \to \omega\gamma)$ ratio*, *Phys. Lett.* **B 487** (2000) 81 [hep-ph/0006054] [INSPIRE].

[8] G. Burdman, E. Golowich, J.L. Hewett and S. Pakvasa, *Radiative weak decays of charm mesons*, *Phys. Rev.* **D 52** (1995) 6383 [hep-ph/9502329] [INSPIRE].

[9] A. Khodjamirian, G. Stoll and D. Wyler, *Calculation of long distance effects in exclusive weak radiative decays of B meson*, *Phys. Lett.* **B 358** (1995) 129 [hep-ph/9506242] [INSPIRE].

[10] S. Fajfer, S. Prelovsek and P. Singer, *FCNC transitions $c \to u\gamma$ and $s \to d\gamma$ in $B_c \to B_u^*\gamma$ and $B_s \to B_d^*\gamma$ decays*, *Phys. Rev.* **D 59** (1999) 114003 [*Erratum ibid.* **D 64** (2001) 099903] [hep-ph/9901252] [INSPIRE].

[11] S. de Boer and G. Hiller, *Flavor and new physics opportunities with rare charm decays into leptons*, *Phys. Rev.* **D 93** (2016) 074001 [arXiv:1510.00311] [INSPIRE].

JHEP08(2017)091

[12] A. Paul, I.I. Bigi and S. Recksiegel, *On $D \to X_u \ell^+ \ell^-$ within the Standard Model and frameworks like the littlest Higgs model with T parity*, *Phys. Rev.* **D 83** (2011) 114006 [arXiv:1101.6053] [INSPIRE].

[13] S. Fajfer, S. Prelovsek and P. Singer, *Rare charm meson decays $D \to P\ell^+\ell^-$ and $c \to u\ell^+\ell^-$ in SM and MSSM*, *Phys. Rev.* **D 64** (2001) 114009 [hep-ph/0106333] [INSPIRE].

[14] S.W. Bosch and G. Buchalla, *The radiative decays $B \to V\gamma$ at next-to-leading order in QCD*, *Nucl. Phys.* **B 621** (2002) 459 [hep-ph/0106081] [INSPIRE].

[15] BELLE collaboration, A. Abdesselam et al., *Observation of $D^0 \to \rho^0\gamma$ and search for CP violation in radiative charm decays*, *Phys. Rev. Lett.* **118** (2017) 051801 [arXiv:1603.03257] [INSPIRE].

[16] LHCb collaboration, *Measurement of the difference of time-integrated CP asymmetries in $D^0 \to K^-K^+$ and $D^0 \to \pi^-\pi^+$ decays*, *Phys. Rev. Lett.* **116** (2016) 191601 [arXiv:1602.03160] [INSPIRE].

[17] S. de Boer, B. Müller and D. Seidel, *Higher-order Wilson coefficients for $c \to u$ transitions in the Standard Model*, *JHEP* **08** (2016) 091 [arXiv:1606.05521] [INSPIRE].

[18] Z.-G. Zhao et al., *Report of Snowmass* 2001 *working group E2: electron-positron colliders from the ϕ to the Z*, *eConf* **C 010630** (2001) E2001 [hep-ex/0201047] [INSPIRE].

[19] D. d'Enterria, *Physics case of FCC-ee*, *Frascati Phys. Ser.* **61** (2016) 17 [arXiv:1601.06640] [INSPIRE].

[20] A. Ali and A.Y. Parkhomenko, *Branching ratios for $B \to K^*\gamma$ and $B \to \rho\gamma$ decays in next-to-leading order in the large energy effective theory*, *Eur. Phys. J.* **C 23** (2002) 89 [hep-ph/0105302] [INSPIRE].

[21] M. Beneke, T. Feldmann and D. Seidel, *Systematic approach to exclusive $B \to V\ell^+\ell^-, V\gamma$ decays*, *Nucl. Phys.* **B 612** (2001) 25 [hep-ph/0106067] [INSPIRE].

[22] M. Beneke, T. Feldmann and D. Seidel, *Exclusive radiative and electroweak $b \to d$ and $b \to s$ penguin decays at NLO*, *Eur. Phys. J.* **C 41** (2005) 173 [hep-ph/0412400] [INSPIRE].

[23] BELLE collaboration, A. Heller et al., *Search for $B^+ \to \ell^+\nu_\ell\gamma$ decays with hadronic tagging using the full Belle data sample*, *Phys. Rev.* **D 91** (2015) 112009 [arXiv:1504.05831] [INSPIRE].

[24] G.P. Korchemsky, D. Pirjol and T.-M. Yan, *Radiative leptonic decays of B mesons in QCD*, *Phys. Rev.* **D 61** (2000) 114510 [hep-ph/9911427] [INSPIRE].

[25] P. Ball and E. Kou, *$B \to \gamma e\nu$ transitions from QCD sum rules on the light cone*, *JHEP* **04** (2003) 029 [hep-ph/0301135] [INSPIRE].

[26] A. Khodjamirian, T. Mannel and N. Offen, *B-meson distribution amplitude from the $B \to \pi$ form-factor*, *Phys. Lett.* **B 620** (2005) 52 [hep-ph/0504091] [INSPIRE].

[27] V. Pilipp, *Matching of λ_B onto HQET*, hep-ph/0703180 [INSPIRE].

[28] S.W. Bosch and G. Buchalla, *Constraining the unitarity triangle with $B \to V\gamma$*, *JHEP* **01** (2005) 035 [hep-ph/0408231] [INSPIRE].

[29] P. Ball, G.W. Jones and R. Zwicky, *$B \to V\gamma$ beyond QCD factorisation*, *Phys. Rev.* **D 75** (2007) 054004 [hep-ph/0612081] [INSPIRE].

[30] A.L. Kagan and M. Neubert, *Isospin breaking in $B \to K^*\gamma$ decays*, *Phys. Lett.* **B 539** (2002) 227 [hep-ph/0110078] [INSPIRE].

JHEP08(2017)091

[31] B. Grinstein, Y. Grossman, Z. Ligeti and D. Pirjol, *The photon polarization in $B \to X\gamma$ in the Standard Model*, *Phys. Rev.* **D 71** (2005) 011504 [hep-ph/0412019] [INSPIRE].

[32] B. Grinstein and D. Pirjol, *Long distance effects in $B \to V\gamma$ radiative weak decays*, *Phys. Rev.* **D 62** (2000) 093002 [hep-ph/0002216] [INSPIRE].

[33] M. Dimou, J. Lyon and R. Zwicky, *Exclusive chromomagnetism in heavy-to-light FCNCs*, *Phys. Rev.* **D 87** (2013) 074008 [arXiv:1212.2242] [INSPIRE].

[34] M. Bauer, B. Stech and M. Wirbel, *Exclusive nonleptonic decays of D, D_s and B mesons*, *Z. Phys.* **C 34** (1987) 103 [INSPIRE].

[35] CLEO collaboration, D.M. Asner et al., *Radiative decay modes of the D^0 meson*, *Phys. Rev.* **D 58** (1998) 092001 [hep-ex/9803022] [INSPIRE].

[36] Particle Data Group collaboration, C. Patrignani et al., *Review of particle physics*, *Chin. Phys.* **C 40** (2016) 100001 [INSPIRE].

[37] A.J. Buras, *QCD factors a_1 and a_2 beyond leading logarithms versus factorization in nonleptonic heavy meson decays*, *Nucl. Phys.* **B 434** (1995) 606 [hep-ph/9409309] [INSPIRE].

[38] H.-Y. Cheng, *Weak annihilation and the effective parameters a_1 and a_2 in nonleptonic D decays*, *Eur. Phys. J.* **C 26** (2003) 551 [hep-ph/0202254] [INSPIRE].

[39] BaBar collaboration, B. Aubert et al., *Measurement of the branching fractions of the radiative charm decays $D^0 \to \bar{K}^{*0}\gamma$ and $D^0 \to \phi\gamma$*, *Phys. Rev.* **D 78** (2008) 071101 [arXiv:0808.1838] [INSPIRE].

[40] J. Lyon and R. Zwicky, *Anomalously large $\mathcal{O}_8$ and long-distance chirality from $A_{CP}[D^0 \to (\rho^0, \omega)\gamma](t)$*, arXiv:1210.6546 [INSPIRE].

[41] G.F. Giudice, G. Isidori and P. Paradisi, *Direct CP-violation in charm and flavor mixing beyond the SM*, *JHEP* **04** (2012) 060 [arXiv:1201.6204] [INSPIRE].

[42] Y. Amhis et al., *Averages of b-hadron, c-hadron and τ-lepton properties as of summer* 2016, arXiv:1612.07233 [INSPIRE].

[43] W. Buchmüller, R. Ruckl and D. Wyler, *Leptoquarks in lepton-quark collisions*, *Phys. Lett.* **B 191** (1987) 442 [*Erratum ibid.* **B 448** (1999) 320] [INSPIRE].

[44] S. Davidson, D.C. Bailey and B.A. Campbell, *Model independent constraints on leptoquarks from rare processes*, *Z. Phys.* **C 61** (1994) 613 [hep-ph/9309310] [INSPIRE].

[45] I. Doršner, S. Fajfer, A. Greljo, J.F. Kamenik and N. Košnik, *Physics of leptoquarks in precision experiments and at particle colliders*, *Phys. Rept.* **641** (2016) 1 [arXiv:1603.04993] [INSPIRE].

[46] G. Hiller, D. Loose and K. Schönwald, *Leptoquark flavor patterns & B decay anomalies*, *JHEP* **12** (2016) 027 [arXiv:1609.08895] [INSPIRE].

[47] M. Carpentier and S. Davidson, *Constraints on two-lepton, two quark operators*, *Eur. Phys. J.* **C 70** (2010) 1071 [arXiv:1008.0280] [INSPIRE].

[48] C. Greub, T. Hurth and D. Wyler, *Virtual $O(\alpha_s)$ corrections to the inclusive decay $b \to s\gamma$*, *Phys. Rev.* **D 54** (1996) 3350 [hep-ph/9603404] [INSPIRE].

[49] L. Lavoura, *General formulae for $f_1 \to f_2\gamma$*, *Eur. Phys. J.* **C 29** (2003) 191 [hep-ph/0302221] [INSPIRE].

JHEP08(2017)091

[50] F. Gabbiani, E. Gabrielli, A. Masiero and L. Silvestrini, *A complete analysis of FCNC and CP constraints in general SUSY extensions of the Standard Model*, *Nucl. Phys.* **B 477** (1996) 321 [hep-ph/9604387] [INSPIRE].

[51] S. Prelovsek and D. Wyler, $c \to u\gamma$ *in the minimal supersymmetric Standard Model*, *Phys. Lett.* **B 500** (2001) 304 [hep-ph/0012116] [INSPIRE].

[52] N. Carrasco et al., D^0-$\bar{D}^0$ *mixing in the Standard Model and beyond from* $N_f = 2$ *twisted mass QCD*, *Phys. Rev.* **D 90** (2014) 014502 [arXiv:1403.7302] [INSPIRE].

[53] M. Frank and S.-Q. Nie, *Chargino contributions to* ϵ'/ϵ *in the left right supersymmetric model*, *J. Phys.* **G 30** (2004) 181 [hep-ph/0306020] [INSPIRE].

[54] G. Hiller and A. Kagan, *Probing for new physics in polarized* Λ_b *decays at the Z*, *Phys. Rev.* **D 65** (2002) 074038 [hep-ph/0108074] [INSPIRE].

[55] A.F. Falk and M.E. Peskin, *Production, decay and polarization of excited heavy hadrons*, *Phys. Rev.* **D 49** (1994) 3320 [hep-ph/9308241] [INSPIRE].

[56] P. Singer and D.-X. Zhang, *Two-body Cabibbo suppressed decays of charmed baryons into vector mesons and into photons*, *Phys. Rev.* **D 54** (1996) 1225 [hep-ph/9603426] [INSPIRE].

[57] P. Böer, T. Feldmann and D. van Dyk, *Angular analysis of the decay* $\Lambda_b \to \Lambda(\to N\pi)\ell^+\ell^-$, *JHEP* **01** (2015) 155 [arXiv:1410.2115] [INSPIRE].

[58] A. Khodjamirian, C. Klein, T. Mannel and Y.-M. Wang, *Form factors and strong couplings of heavy baryons from QCD light-cone sum rules*, *JHEP* **09** (2011) 106 [arXiv:1108.2971] [INSPIRE].

[59] C.-F. Li, Y.-L. Liu, K. Liu, C.-Y. Cui and M.-Q. Huang, *Analysis of the semileptonic decay* $\Lambda_c \to ne^+\nu_e$, *J. Phys.* **G 44** (2017) 075006 [arXiv:1610.05418] [INSPIRE].

[60] T. Gutsche, M.A. Ivanov, J.G. Körner, V.E. Lyubovitskij and P. Santorelli, *Heavy-to-light semileptonic decays of* Λ_b *and* Λ_c *baryons in the covariant confined quark model*, *Phys. Rev.* **D 90** (2014) 114033 [*Erratum ibid.* **D 94** (2016) 059902] [arXiv:1410.6043] [INSPIRE].

[61] R.N. Faustov and V.O. Galkin, *Semileptonic decays of* Λ_c *baryons in the relativistic quark model*, *Eur. Phys. J.* **C 76** (2016) 628 [arXiv:1610.00957] [INSPIRE].

[62] T. Uppal and R.C. Verma, *Weak electromagnetic decays of charm baryons*, *Phys. Rev.* **D 47** (1993) 2858 [INSPIRE].

[63] M. Lisovyi, A. Verbytskyi and O. Zenaiev, *Combined analysis of charm-quark fragmentation-fraction measurements*, *Eur. Phys. J.* **C 76** (2016) 397 [arXiv:1509.01061] [INSPIRE].

[64] M. Galanti, A. Giammanco, Y. Grossman, Y. Kats, E. Stamou and J. Zupan, *Heavy baryons as polarimeters at colliders*, *JHEP* **11** (2015) 067 [arXiv:1505.02771] [INSPIRE].

[65] Y. Kats, *Measuring c-quark polarization in* $W + c$ *samples at ATLAS and CMS*, *JHEP* **11** (2016) 011 [arXiv:1512.00438] [INSPIRE].

[66] E791 collaboration, E.M. Aitala et al., *Mass splitting and production of* Σ_c^0 *and* Σ_c^{++} *measured in* 500 *GeV* $\pi^- n$ *interactions*, *Phys. Lett.* **B 379** (1996) 292 [hep-ex/9604007] [INSPIRE].

[67] CLEO collaboration, G. Brandenburg et al., *Observation of two excited charmed baryons decaying into* $\Lambda_c^+\pi^\pm$, *Phys. Rev. Lett.* **78** (1997) 2304 [INSPIRE].

JHEP08(2017)091

[68] J.G. Korner, A. Pilaftsis and M.M. Tung, *One loop QCD mass effects in the production of polarized bottom and top quarks*, *Z. Phys.* **C 63** (1994) 575 [hep-ph/9311332] [INSPIRE].

[69] K.G. Chetyrkin, J.H. Kuhn and M. Steinhauser, *RunDec: a Mathematica package for running and decoupling of the strong coupling and quark masses*, *Comput. Phys. Commun.* **133** (2000) 43 [hep-ph/0004189] [INSPIRE].

[70] *UTfit collaboration webpage*, http://www.utfit.org/UTfit/.

[71] S. Aoki et al., *Review of lattice results concerning low-energy particle physics*, *Eur. Phys. J.* **C 77** (2017) 112 [arXiv:1607.00299] [INSPIRE].

[72] A. Bharucha, D.M. Straub and R. Zwicky, $B \to V\ell^+\ell^-$ *in the Standard Model from light-cone sum rules*, *JHEP* **08** (2016) 098 [arXiv:1503.05534] [INSPIRE].

[73] CLEO collaboration, S. Dobbs et al., *First measurement of the form factors in the decays* $D^0 \to \rho^- e^+ \nu_e$ *and* $D^+ \to \rho^0 e^+ \nu_e$, *Phys. Rev. Lett.* **110** (2013) 131802 [arXiv:1112.2884] [INSPIRE].

[74] J.M. Flynn and C.T. Sachrajda, *Heavy quark physics from lattice QCD*, *Adv. Ser. Direct. High Energy Phys.* **15** (1998) 402 [hep-lat/9710057] [INSPIRE].

[75] UKQCD collaboration, J. Gill, *Semileptonic decay of a heavy light pseudoscalar to a light vector meson*, *Nucl. Phys. Proc. Suppl.* **106** (2002) 391 [hep-lat/0109035] [INSPIRE].

[76] BESIII collaboration, M. Ablikim et al., *Measurement of the form factors in the decay* $D^+ \to \omega e^+ \nu_e$ *and search for the decay* $D^+ \to \phi e^+ \nu_e$, *Phys. Rev.* **D 92** (2015) 071101 [arXiv:1508.00151] [INSPIRE].

[77] Y.-L. Wu, M. Zhong and Y.-B. Zuo, $B_{(s)}$, $D_{(s)} \to pi$, K, η, ρ, K^*, ω, ϕ *transition form factors and decay rates with extraction of the CKM parameters* $|V_{ub}|$, $|V_{cs}|$, $|V_{cd}|$, *Int. J. Mod. Phys.* **A 21** (2006) 6125 [hep-ph/0604007] [INSPIRE].

[78] D. Melikhov and B. Stech, *Weak form-factors for heavy meson decays: an update*, *Phys. Rev.* **D 62** (2000) 014006 [hep-ph/0001113] [INSPIRE].

[79] R.C. Verma, *Decay constants and form factors of s-wave and p-wave mesons in the covariant light-front quark model*, *J. Phys.* **G 39** (2012) 025005 [arXiv:1103.2973] [INSPIRE].

[80] S. Fajfer and J.F. Kamenik, *Charm meson resonances and* $D \to V$ *semileptonic form-factors*, *Phys. Rev.* **D 72** (2005) 034029 [hep-ph/0506051] [INSPIRE].

[81] J. Charles, A. Le Yaouanc, L. Oliver, O. Pene and J.C. Raynal, *Heavy to light form-factors in the heavy mass to large energy limit of QCD*, *Phys. Rev.* **D 60** (1999) 014001 [hep-ph/9812358] [INSPIRE].

[82] R. Casalbuoni, A. Deandrea, N. Di Bartolomeo, R. Gatto, F. Feruglio and G. Nardulli, *Effective Lagrangian for heavy and light mesons: semileptonic decays*, *Phys. Lett.* **B 299** (1993) 139 [hep-ph/9211248] [INSPIRE].

[83] P.L. Cho and M.B. Wise, *Comment on* $D_s^* \to D_s \pi^0$ *decay*, *Phys. Rev.* **D 49** (1994) 6228 [hep-ph/9401301] [INSPIRE].

[84] A.J. Buras, A. Czarnecki, M. Misiak and J. Urban, *Completing the NLO QCD calculation of* $\bar{B} \to X_s \gamma$, *Nucl. Phys.* **B 631** (2002) 219 [hep-ph/0203135] [INSPIRE].

JHEP08(2017)091